REPORT DOCUMENTATION PAGE

Form Approved
OMB No. 0704-0188

1. AGENCY USE ONLY (Leave blank)	2. REPORT DATE	3. REPORT TYPE AND DATES COVERED
	10 Sep 95	

4. TITLE AND SUBTITLE
A Study of Lightning Activity Over The Warm Pool Western Pacific Ocean (Toga-Coare Region For 1993

5. FUNDING NUMBERS

6. AUTHOR(S)
Luis Alberto Rios

7. PERFORMING ORGANIZATION NAME(S) AND ADDRESS(ES)
AFIT Students Attending:
Texas A&M University

8. PERFORMING ORGANIZATION REPORT NUMBER
95-115

9. SPONSORING/MONITORING AGENCY NAME(S) AND ADDRESS(ES)
DEPARTMENT OF THE AIR FORCE
AFIT/CI
2950 P STREET, BLDG 125
WRIGHT-PATTERSON AFB OH 45433-7765

10. SPONSORING/MONITORING AGENCY REPORT NUMBER

11. SUPPLEMENTARY NOTES

12a. DISTRIBUTION/AVAILABILITY STATEMENT
Approved for Public Release IAW AFR 190-1
Distribution Unlimited
BRIAN D. GAUTHIER, MSgt, USAF
Chief of Administration

12b. DISTRIBUTION CODE

13. ABSTRACT *(Maximum 200 words)*

19951017 158

14. SUBJECT TERMS	15. NUMBER OF PAGES 97
	16. PRICE CODE

17. SECURITY CLASSIFICATION OF REPORT	18. SECURITY CLASSIFICATION OF THIS PAGE	19. SECURITY CLASSIFICATION OF ABSTRACT	20. LIMITATION OF ABSTRACT

A STUDY OF LIGHTNING ACTIVITY OVER THE WARM POOL WESTERN PACIFIC OCEAN (TOGA-COARE REGION) FOR 1993

A Thesis

by

LUIS ALBERTO RIOS

Submitted to Texas A&M University
in partial fulfillment of the requirements
for the degree of

MASTER OF SCIENCE

Approved as to style and content by:

Richard E. Orville
(Chair of Committee)

John F. Griffiths
(Member)

H. Joseph Newton
(Member)

Edward J. Zipser
(Head of department)

May 1995

Major Subject: Meteorology

ABSTRACT

A Study of Lightning Activity Over the Warm Pool Western Pacific Ocean (TOGA-COARE Region) for 1993. (May 1995)

Luis Alberto Rios, B. S., Rutgers University

Chair of Advisory Committee: Dr. Richard E. Orville

The warm pool western Pacific Ocean is an area of the equatorial tropics characterized by strong and frequent convection, and vigorous lightning activity. However, it has been noted by various researchers that the vast oceanic expanses experience less lightning activity than adjacent land masses by as much as one order of magnitude. A report herein presents a look at the characteristics of lightning as recorded by three individual magnetic direction finders (DF's) at the Kapingamarangi Atoll, Rabaul, and Kavieng deployed to the Tropical Ocean Global Atmosphere Coupled Ocean-Atmosphere Response Experiment (TOGA-COARE).

The lightning data recorded by each DF are azimuthally separated into "land" and "ocean" sectors in an effort to assess each regimes similarities and differences. In addition to analyzing some of the more typical lightning parameters (e.g., percentage of positive lightning and positive and negative multiplicities), the thermodynamic relationships between convective available potential energy (CAPE), wet-bulb potential temperature, and flash rates are examined. Finally, the lightning data are run through time series methods in an attempt to both better describe the data and to appraise any possible link between lightning activity and the Madden-Julian Oscillation (MJO) through the use of an appropriately constructed band-pass filter.

The results show that lightning activity in this region is remarkably biased towards land masses with land/ocean lightning ratios often exceeding 10. Figures on the percentage of positive lightning and positive/negative multiplicities agree well with results from United States studies in pattern though not in average values. Also, diurnal variation of lightning activity over the TOGA-COARE region is dramatically different from that of a typical United States locale with a pronounced maximum in activity that occurs between roughly 2000 and 0500 local standard time (LST).

The relationship between CAPE and flash rate was not observed to be as well defined as previously suggested, pointing to possible limitations in the thermodynamic data, CAPE computation procedures and to parcel theory pitfalls. Finally, the construction of a band-pass filter to study the possible link between lightning activity and the MJO reveals a subtle link which is best seen during the Northern Hemisphere winter and spring months.

DEDICATION

I would like to dedicate this thesis to several people. First of all, to my family for their unending love, support, encouragement, and prayers. Also, I dedicate this thesis to my many brothers and sisters in the Lord Jesus Christ whom I have come to love and depend on for support through many of life's trials.

Finally, I'd like to dedicate this thesis to my Lord and Savior Jesus Christ, "...the author and perfecter of my faith..." (Hebrews 12:2)

ACKNOWLEDGMENTS

First, and foremost, thanks be to God.

I would like to thank the members of my committee, Dr. Richard E. Orville and Dr. H. Joseph Newton and Professor John F. Griffiths for their guidance and support during my research. Special thanks go to Dr. Orville for his help in choosing and focusing the objectives of my research and to the United States Air Force for financially supporting me through my graduate studies while at Texas A&M University.

I want also to thank several faculty members and fellow graduate students for their invaluable assistance. Specifically, I would like to thank Dr. Ilya Polyak and Dr. Kwang-Yul Kim for their help with computer programs used in the analysis of some of my data. Mr. Christopher Lucas, Mr. Stephen Barnaby, and Mrs. Donna Smith were instrumental in the analysis of the lightning data as well as providing valuable meteorological advice. Thanks also to the Lightning Group/Dr. Zipser students whose assistance helped avoid countless hours of frustration. Finally, I would like to acknowledge my good friends and Air Force peers Bill Carle and Tony Moninski for being there for me in general.

TABLE OF CONTENTS

CHAPTER Page

LIST OF TABLES

LIST OF FIGURES

FIGURE Page

CHAPTER I

INTRODUCTION

One of the most highly researched yet poorly understood of all the phenomena in atmospheric physics and meteorology is lightning. Nowhere is such a research effort more evident than within the warm pool western Pacific Ocean. The warm pool western Pacific Ocean is an area of the deep equatorial tropics characterized by sea surface temperatures that, on average, exceed 28°C. In addition, the area experiences heavy precipitation (>3,000 mm over most of the area) as well as strong, frequent convection, and vigorous lightning activity (Webster and Lukas 1992). The region of the tropics to be examined in this study encompasses the waters just north of northeastern Australia and south of Micronesia. Previous research suggests that although this area is prone to intense and deep convective activity, the vast oceanic expanses experience less lightning activity than land masses by as much as an order of magnitude (Takahashi 1978a, 1990; Rutledge et al. 1992; Williams et al. 1992).

The main objective of this investigation is to provide a picture of the pattern that lightning activity exhibits over this part of the tropics. This will be accomplished through the study of data collected by three magnetic direction finders (DF's) during 1993. These data were obtained as part of the Tropical Ocean and Global Atmospheric-Coupled Ocean Atmospheric Response Experiment (TOGA-COARE)

The citations on this and subsequent pages follow the style of the *Monthly Weather Review.*

and include twelve months of lightning data for both Rabaul and Kavieng and six and a half months (1 January - 14 July 1993) for the Kapingamarangi Atoll. Previous research efforts into the nature of tropical lightning were limited by temporal and spatial constraints. Lightning studies in and around the warm pool western Pacific prior to TOGA-COARE include the work of Thomson (1980) in Port Moresby, Papua New Guinea, Rutledge et al. (1992) near Darwin, Australia and the electrification experiments conducted by Takahashi in Ponape, Micronesia (1978, 1990). Although thorough in procedure, these experiments lacked the continuity and coverage quality that the TOGA-COARE data sets provide.

Rather than superficially analyzing the many possible parameters available within the lightning data sets, a more thorough examination of several of them is conducted. Additionally, the continuity and length of the data sets allow for the rigorous comparison of this investigation's findings with those of previous works which had smaller data bases with which to work. It is extremely important to note that careful consideration will be given to the fact that the 1-DF TOGA-COARE data suffer from an increased degree of contamination. This stems from the increase in range of each DF from 400 km to approximately 900 km. Although no figures on detection efficiencies for the TOGA-COARE DF's currently exist, attention to intracloud waveform contamination have to be addressed in conjunction with any findings that are obtained through the course of this investigation (Orville et al. 1994).

The breadth of the study be broken up into three sections. (1) First, the lightning data are analyzed from the standpoint of land versus ocean differences. The range

area of each DF is broken up into "land" and "ocean" sectors (methodology adapted from Lucas and Orville 1994) which facilitates analysis of azimuthal distributions of lightning, for example. By breaking up each range's area into sectors, ***an estimate*** of each DF's land:ocean lightning ratio can be computed for each month. The aforementioned sectoring also allows for the the analysis of such parameters as multiplicities, percentage of positive lightning, as well as land and ocean diurnal cycles. The intent is that further insight may be gained into the behavior of lightning within the TOGA-COARE region.

(2) An analysis of the lightning data against various thermodynamic parameters such as convective available potential energy (CAPE), convective inhibition energy (CINE), and wet bulb potential temperature (θ_w) comprises the second section. Of interest is the spatial and temporal distribution of CAPE and θ_w observed through data gathered at the following TOGA-COARE stations: Nauru, Kapingamarangi, Kavieng and Manus Island. These stations provide coverage from east to west through the Outer Soundings Array (OSA) and the Intensive Flux Array (IFA). In addition, comparisons would be made using lightning locations obtained from a multi-DF analysis. With the aid of the *XLIGHT* display software, lightning activity around Kapingamarangi and Kavieng is isolated for each day of the latter half of the Intensive Observation Period (IOP; 1 January - 28 February 1993) and examined against the previously mentioned thermodynamic parameters.

(3) The final step in the analysis of these data is to perform a more sophisticated statistical analysis using time series methods. Time series methods allow for the

detailed description of data sets in addition to suggesting statistical models with which to simulate and forecast the data. The basis for performing time series analysis on this particular set of data stems from the fact that it may exhibit serial correlation, that is, correlation over time (Newton 1988). Of particular interest is a spectral analysis of the lightning flash totals at all three locales using the 1-DF data sets in order to investigate whether or not a link does indeed exist to the so called Madden-Julian Oscillation (MJO).

CHAPTER II

BACKGROUND

1. TOGA-COARE Overview

With the need to establish a physical basis for the phenomenon of climate change and the development and advancements of coupled ocean-atmosphere models, the international community launched the Tropical Ocean-Global Atmosphere (TOGA) program as part of the World Climate Research Programme (WCRP) in 1985 (Webester and Lukas 1992). Despite the vast amounts of data obtained as a result of TOGA, considerable scientific objectives remained virtually unexplained.

Chief among these are the mechanisms responsible for coupling the oceanic basin and the atmosphere in the warm pool western Pacific and the principal processes by which convection is organized in this region. In an effort to better understand the above objectives, the TOGA Coupled Ocean-Atmosphere Response Experiment (TOGA-COARE) was set in motion and developed in three components; interface, atmospheric and oceanographic. The layout of the experiment allowed for complex in situ measurements of many meteorological and oceanographic parameters spanning the period 1 November 1992 through 28 February 1993. This period, known as the IOP, was followed by a time interval of enhanced monitoring which continued throughout 1993 (Webster and Lukas 1992). Coincidentally, when the COARE "arm" of TOGA became operational in November of 1992, a serious effort was set into

motion to study the electrical properties of cloud systems in this active part of the equatorial tropics.

2. Survey of Literature

Although significant and extensive efforts have characterized lightning research over the mid latitudes, the deep tropics have lacked a commensurate amount of study. With the advent of new technologies and the need to understand better the subtle, yet powerful, link between the tropical ocean and the atmosphere, lightning research has recently flourished in this part of the world.

To the untrained observer, it would seem, that lightning occurs over the tropical regime with little, if any, difference between the land and its adjacent waters. This, however, is not the case. The availability and use of more sophisticated satellites and their data, have made it possible to obtain estimates of lightning on a global scale. The findings of such efforts have puzzled researchers for some time now. For example, Orville and Henderson (1986) used the high resolution scanner on board the Defense Meteorological Satellite Program (DMSP) F1 satellite to obtain a distribution of global midnight lightning from 60°S to 60°N (Fig. 1). Although the detected amount is a mere fraction of the total count, the authors stress that it is the relative number of flashes that matters and not the absolute total. Cursory examination of Fig. 1 reveals the significant difference in lightning that obviously exists between the land and the ocean. After correcting for earth's land to ocean ratio of 2.4, an annual ratio of land versus ocean lightning of 7.7 was calculated (Orville and Henderson 1986).

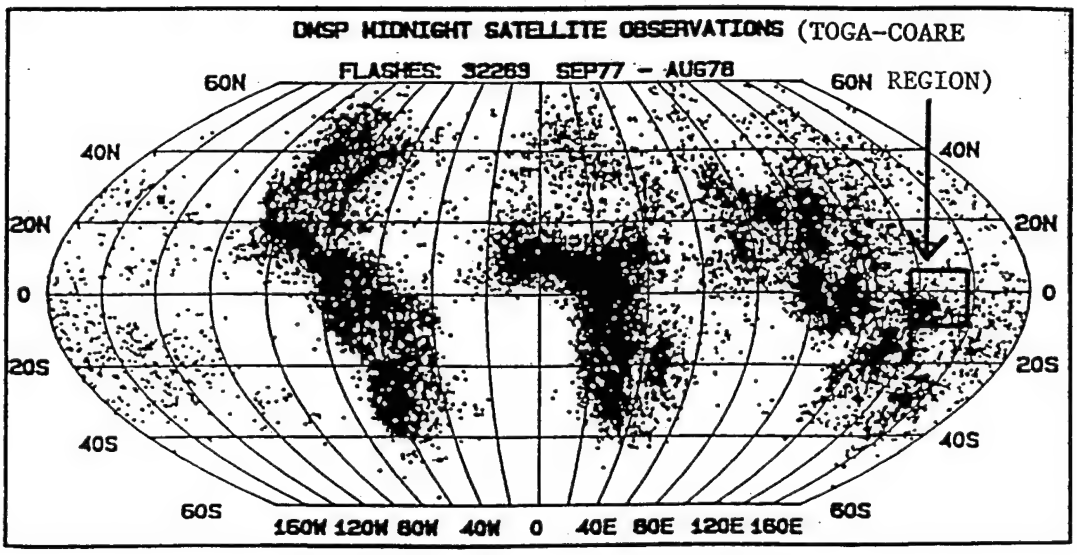

Fig. 1 DMSP satellite observations of global midnight lightning. Total number of flashes with political and land/sea boundaries removed (Adapted from Orville and Henderson 1986).

In a preliminary study of the Kavieng TOGA COARE lightning data, Lucas and Orville (1994) show a similar ratio of 8.7. In spite of its comprehensive nature, this study cannot answer the question of why the marked difference in lightning between the land and the ocean occurs. Other studies, while focusing on other parameters have dealt with the same basic issue.

Of special interest in the warm pool Western Pacific (but also throughout the tropical oceans) is understanding of the many scales and forms of convection (Webster and Lukas 1992). Although tropical mesoscale and convective scale disturbances can, and often do, reach the tropical tropopause, lightning activity over the water is dramatically weak (Rutledge et al. 1992; Williams et al 1992; Zipser 1994). Takahashi (1978a), for example, focused part of his research on weakly electrified cloud systems

near Ponape, Micronesia (north-northeast of the TOGA-COARE region [7°N, 158°E]). Based on experimental data gathered at Ponape, Takahashi proposes that thunderstorms acquire electrical charge primarily from charge separation during graupel formation. He emphasizes that the sign and magnitude of the charge depends on temperature and supercooled cloud liquid water content (Takahashi 1978a,b).

To this day, no single theory on cloud electrification is considered conclusive. However, examination of the theories which result in electric fields capable of producing lightning suggests that "the noninductive charge transfer occurring when ice crystals collide with and separate from a riming hailstone is the primary candidate to explain thunderstorm electrification" (Illingworth 1985). This issue continues to be at the center of lightning research as understanding charging mechanisms is deemed essential in solving many of the mysteries often associated with the phenomenon. As stated by Williams (1989), "the understanding of electric charge transfer in ice particle collisions is the outstanding problem in cloud electrification today." Regardless, it is generally recognized by the scientific community that thunderstorms are directly responsible for maintaining a negative charge on the earth. This aspect of thunderstorms, better known as the global circuit, is accomplished, in bulk, through lightning discharges (Saunders 1988).

Although Orville and Henderson's (1986) satellite estimates of midnight lightning suggest a significant difference between lightning frequencies over the land and over the oceans, no ***thorough*** studies of this curious fact had been conducted in this area prior to the Down Under Doppler Electricity Experiment (DUNDEE; Rutledge et al.

1992; Randell et al. 1994). During the wet seasons of 1988-89 and 1989-90 (November through January) the DUNDEE was conducted in and around Darwin, Australia. Its location afforded the opportunity to examine the dynamical and electrical differences of lightning activity from both a continental and maritime point of view. Rutledge et al. (1992) and Williams et al. (1992), for example, theorize that lightning in this area, and variations of it, are linked to monsoon trough activity versus "break period" activity (i.e. the break in the persistent low level westerlies [~850 mb] which help drive the monsoon). Specifically, they point to the availability of convective available potential energy (CAPE) as a significant lightning enhancer. Rutledge et al. (1992) conclude that monsoon periods (characterized by low values of CAPE), and their attendant widespread precipitation patterns, experience low lightning rates, while break periods (characterized by high values of CAPE), and their more widely isolated convection experience high lightning rates.

Expanding on the CAPE/storm electrification relationship, Randell et al. (1994), conducted numerical modeling studies of low, moderate and high CAPE environments. They conclude that a comparison of the three types of simulations suggests a correlation between CAPE, strength and rate of electrification consistent with observations from the DUNDEE (Rutledge et al. 1992, Williams et al. 1992). Central to the findings of Randell et al. (1994) is the idea that storm electrification is observed to be critically dependent on the positioning of the level of charge reversal (LCR), which is itself dependent on cloud temperature, liquid water content and the particle interaction region. This region (a.k.a. the mixed phase region) is where ice particle

collisions take place and where ***non-inductive*** charge separation can occur (Takahashi 1978b).

Others, however, have narrowed their attention to explaining, in detail, the thermodynamics behind CAPE calculations and procedures in order to point out the many pitfalls intrinsic to parcel theory (Williams et al. 1992; Williams and Renno 1993). In reviewing the Darwin data (DUNDEE), Williams et al. (1992) stress the ambiguity of CAPE calculations which are particularly apparent during monsoon periods. During the aforementioned periods, the calculated values were often as large as the possible error in CAPE computation. This points to the difficulty of proper acquisition of representative soundings during monsoon episodes. During break periods, on the other hand, high CAPE values have been shown to be quite representative of the preconvective environmental conditions which eventually lead to vigorous lightning activity (Rutledge et al. 1992).

In an analysis of the conditional stability of the tropical atmosphere, Williams and Renno (1993) show that out of the three possible CAPE computation procedures (*pseudoadiabatic, reversible and reversible with ice*), the reversible with ice method often yields more realistic results. Using this method they found that the negative buoyancy created by water loading is offset by the release of latent heat of freezing. Other interesting findings include a well correlated linear relationship between CAPE and the wet bulb potential temperature (moist entropy) of the boundary layer and the role of CINE. Data from Ponape, Darwin and Belem (Brazil) show that θ_w appears to be a reliable proxy to CAPE with a well defined zero-CAPE intercept near 22°C-23°C.

Although the moist entropy and CAPE relationship is well accepted, the paradox remains. Oceanic convection is likely to be weakly electrified, in spite of the fact that it occurs amidst a massive storehouse of energy (i.e. the tropical ocean-atmosphere couplet).

Assuming CAPE is a reliable indicator of the potential vigor of lightning activity is not necessarily prudent. For example, Xu and Emanuel (1989) point out that large amounts of CAPE can and do build in the tropics without being released. They point to the presence of strong capping inversions as a significant barrier to the lifting of near-surface air to its level of free convection (LFC). In addition, the vertical velocity which could be attained by a complete conversion of the CAPE into an updraft, is generally believed to be a "...gross overestimate of the true vertical velocity for most conditions." This essentially renders CAPE as an overly simplistic measure of convective instability (Lucas et al. 1994a). LeMone et al. (1994) note that buoyancies at lower levels (< 6 km) tend to be significantly higher over the more strongly heated land than over the oceans. There are stronger and larger updrafts over land masses even if land and ocean CAPE's are similar.

Interestingly, the set of lightning data collected over the Western Pacific has also shown a periodicity in the 30-40 day range (Lucas and Orville 1994). Although this finding is that of a ***limited time series*** of flash totals, it may be indicative of the 40-60 day oscillation first described by Madden and Julian (1971, 1972) and most recently summarized by Madden and Julian (1994). This feature is one in which an oscillation

of long period (~41-53 days) appeared in the station pressure, temperature and zonal wind components at Canton Island (3°S, 172°W, now known as Kanton).

In their 1972 paper, Madden and Julian insist that in order to drive and sustain the so-called oscillation, a very large source of energy is needed. Ramage (1968) shows how the "maritime continent" (a.k.a. the warm pool Western Pacific) provides the necessary energy through convection. They propose that the oscillation is a large circulation cell oriented in zonal planes and centered in the mid-Pacific Ocean which essentially serves to enhance convection over the tropics.

More recent studies examining anomalies in outgoing longwave radiation (OLR) patterns using satellite data have shown modulations on the convection cycle over this part of the tropics but with a slightly different period. Knutson and Weickmann (1987) have shown how large-scale tropical divergent wind flows and OLR anomalies (negative anomalies implying more convection) propagate eastward in time with a characteristic time scale of 30 to 60 days. These features are seen to be strongest within 20 degrees of the equator and over the Indian and western Pacific Oceans.

CHAPTER III

DATA

1. Sources and Limitations

The lightning data gathered at Rabaul, Kavieng, and the Kapingamarangi Atoll were collected by magnetic direction finders (DF's) that were especially altered for TOGA-COARE. Specifically, these data include azimuth angle, polarity, and time of occurrence (to the nearest microsecond) of each flash. Although signal strength and peak electric field are also available, they are not used in this study. Because of in situ problems with equipment during the course of the experiment, some daily tallies of lightning data are not available. Specifically, all the May 28 lightning is missing from the Kavieng data set while Kapingamarangi lacks June 12th and 13th. Rabaul's data gap encompasses a more significant period of time. Altogether, seventeen days in October and one in November are missing.

In order to survey as large an area as possible, the gain of each DF was increased from its normal 400 km to a nominal range of approximately 900 km. This special modification was made to attain the desired increase in detection range while maintaining a ***relatively*** low degree of contamination from intracloud waveforms (Orville et al. 1993). One significant drawback which is introduced by the gain modification is that as the range increases, so does the sensitivity of each DF to the larger amplitude intracloud wave forms. The increase in gain not only leads to an overestimation of the total number of flashes, but also lowers the detection efficiency

of each finder (Orville et al. 1993). It is imperative to mention that no figures on detection efficiencies have yet been computed for the three DF's deployed in the TOGA-COARE area. Unfortunately, efficiencies recorded using existing finders in the United States cannot be used even as a rough guide as a result of the many differences in equipment set-up and location over which the DF's were deployed. Marx Brook, of The New Mexico Institute of Technology, is currently working towards obtaining TOGA-COARE DF efficiencies. This limitation notwithstanding, it is worth mentioning that efficiencies in the United States have been found at roughly 70% in Oklahoma (Mach et al. 1986), Albany and the NASA Kennedy Space Center (KSC; Orville et al. 1987) using summer measurements. Other estimates using the high gain detectors at the KSC by Maier (1991) show that efficiencies can vary from a low of 53% to a high of 72%, for example. It should be interesting to see how these compare to those computed for the TOGA-COARE region.

In addition to affecting the detection efficiencies, the increase in range also demands that attention be focused on the polarity figures obtained. As shown by Brook et al. (1989), the polarity of lightning flashes detected by a DF beyond 600 km may be incorrect. Outside this critical distance, a DF may record ionospheric reflections, whose waveforms are inverted. The result of this atmospheric phenomenon is an incorrect polarity measurement.

The sounding data used in the thermodynamic analysis were collected by four Integrated Sounding System (ISS) profilers deployed to Kapingamarangi, Kavieng, Manus Island, and Nauru. Temporal coverage for Kapingamarangi, Manus Is., and

Nauru includes January 1993 through June 1993 while the Kavieng profiler was in operation from January 1993 through February 1993. At all locations, thermodynamic data are available for 11 and 23 UTC (for January through June) and 05, 11, 17 and 23 UTC during the IOP months of January and February.

More precisely, the sounding data are National Center for Atmospheric Research (NCAR) class sounding data available via anonymous ftp in ASCII format. A specific limitation of the thermodynamic data, however, is the fact that an error in the humidity values at low levels was discovered resulting from extraneous cooling and heating of the sensor arm prior to the launching of the sounding. These erroneously low humidity measurements were seen to persist for approximately 40 seconds after launch. Thereafter, the sensor arm came into quasi-equilibrium with the environment, essentially solving the problem. As a result, CAPE, CINE and other low level humidity variables (θ_w, for example) will be consider preliminary at this point and reexamined upon collection of the newer, corrected data set. Figure 2 shows the locations where all three DF's were deployed to as well as all four chosen ISS sites (with respect to the OSA bounds).

One final, and significant, limitation of the thermodynamic data is the way in which they are analyzed. In order to compute CAPE, CINE and other surface parameters, the data are read into the NCAR System for User-editing and Display Software (SUDS) analysis package. In addition to computing time-period specific lists of thermodynamic parameters, the program provides a hard copy of each day's skew-T.

The significant limitation placed on the data centers around the thermodynamic and microphysical

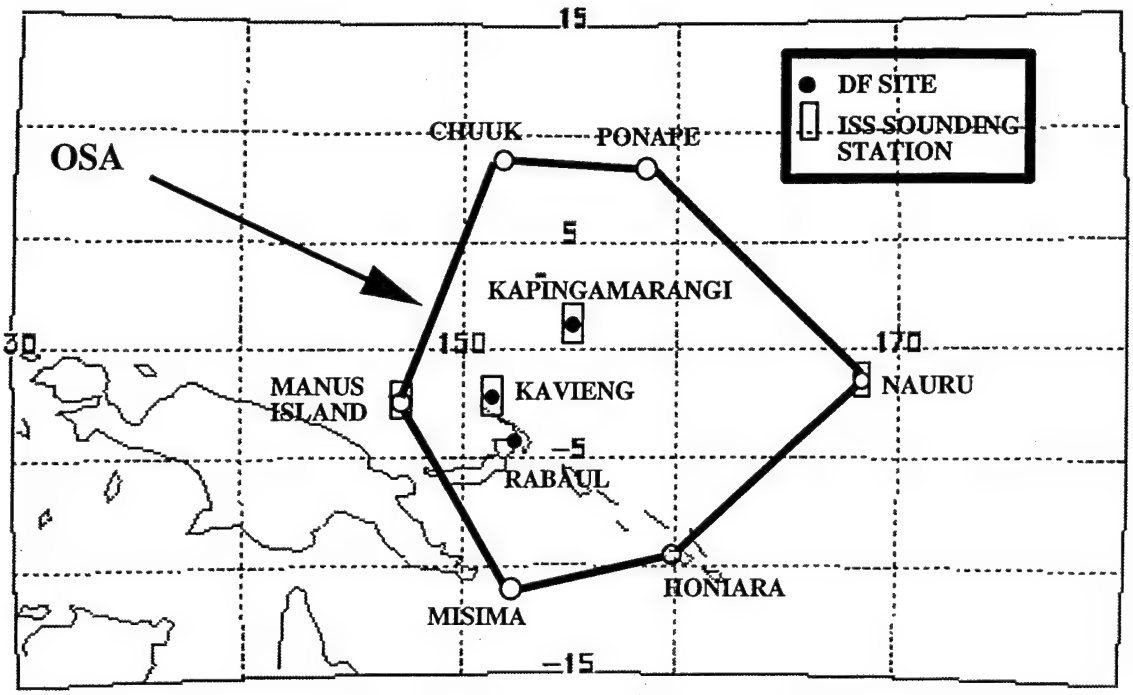

Fig. 2. Direction finder and sounding station locations used during this investigation. Solid circles represent DF's while open rectangles represent sounder locations.

assumptions. Williams and Renno (1993), for example, state how the choice of procedure is often crucial. The SUDS software package used in this investigation assumes the more "typical" irreversible or pseudoadiabatic process where all the liquid water condensate is assumed to immediately "fall out" from the rising parcel upon formation. This assumption eliminates the need to take into account the heat content of the condensed material. Also, the question of sublimation, and when it becomes important, is avoided as well.

The outgoing longwave radiation (OLR) anomaly data used in this study comes from the Climatic Diagnostic Bulletin, December 1993 issue. These data were both spatially and temporally smoothed into a time and longitude diagram (known as a Hovmoller diagram). The motivation behind using these smoothed data stems from the fact that clouds (the source of OLR) inherently display a very high degree of variability from day-to-day and even from cloud element to cloud element. As a result, it is necessary to average out the data in order to obtain any type usable pattern. Specifically, the data are averaged per five-day period (known as a pentad) between 5°N and 5°S for the entire circumference of the earth.

2. Processing

The DF data available for this study are in ASC-II format, and, with the exception of the aforementioned missing days, it were carefully screened for bogus data lines, misplaced alphanumeric characters, and temporal completeness. These data were then read into a C program which summarized the data into daily, hour by hour and azimuthal flash tallies.

Specific to the analysis of the 1-DF data sets is the classification of lightning flashes into "land" and "ocean" sectors. This is based on azimuthal sectors chosen as representative of the land and ocean regimes. Figures 3a-c shows the azimuthal breakdown at all three DF sites. Kapingamarangi's sectors (Fig. 3a) shows that land flashes encompass those flashes recorded from 150° clockwise through 269° while ocean flashes unambiguously comprise the rest of the area. Figure 3b shows

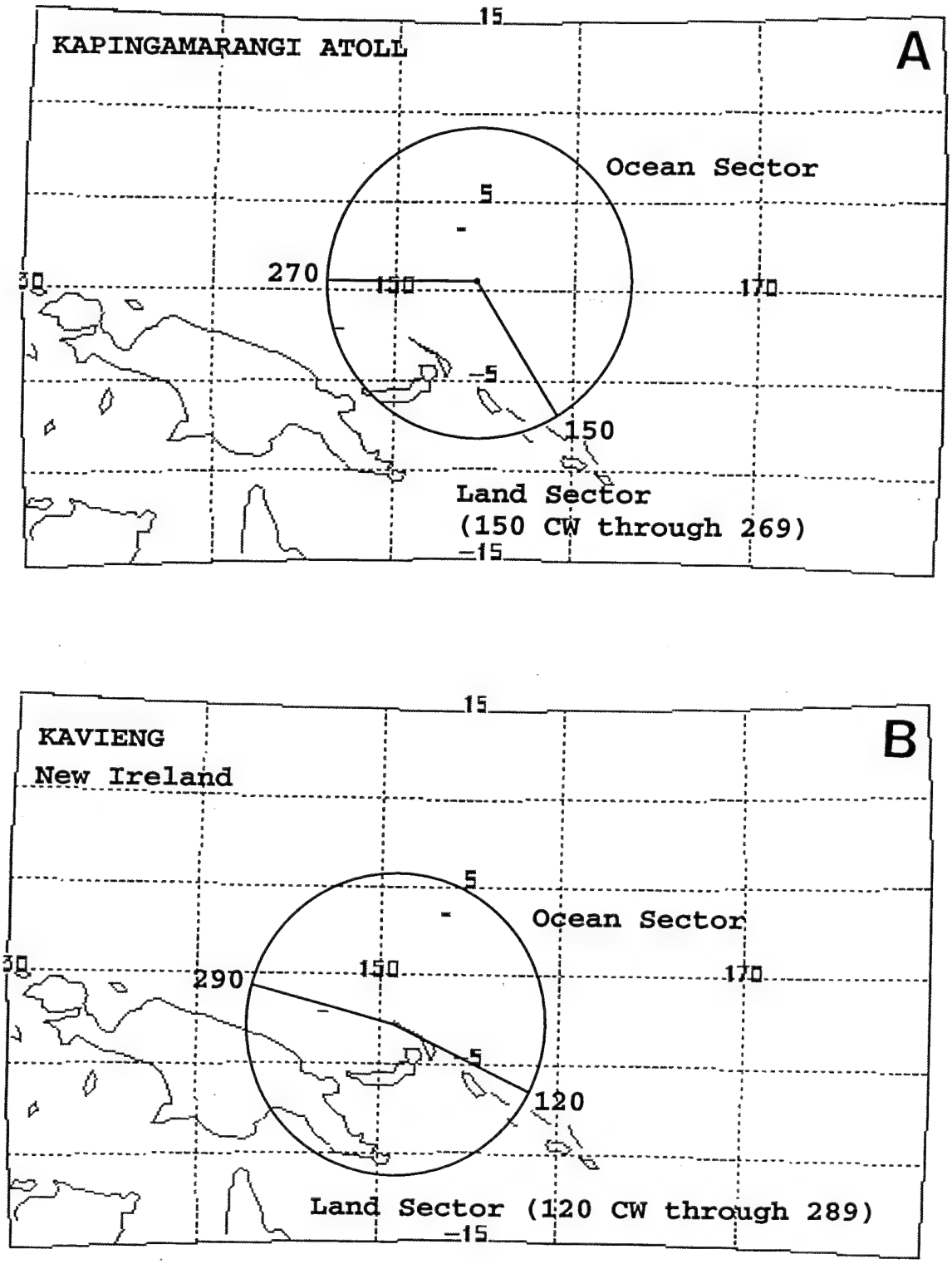

Fig. 3. Land/ocean sector break-ups for (a) Kapingamarangi, (b) Kavieng, and (c) Rabaul.

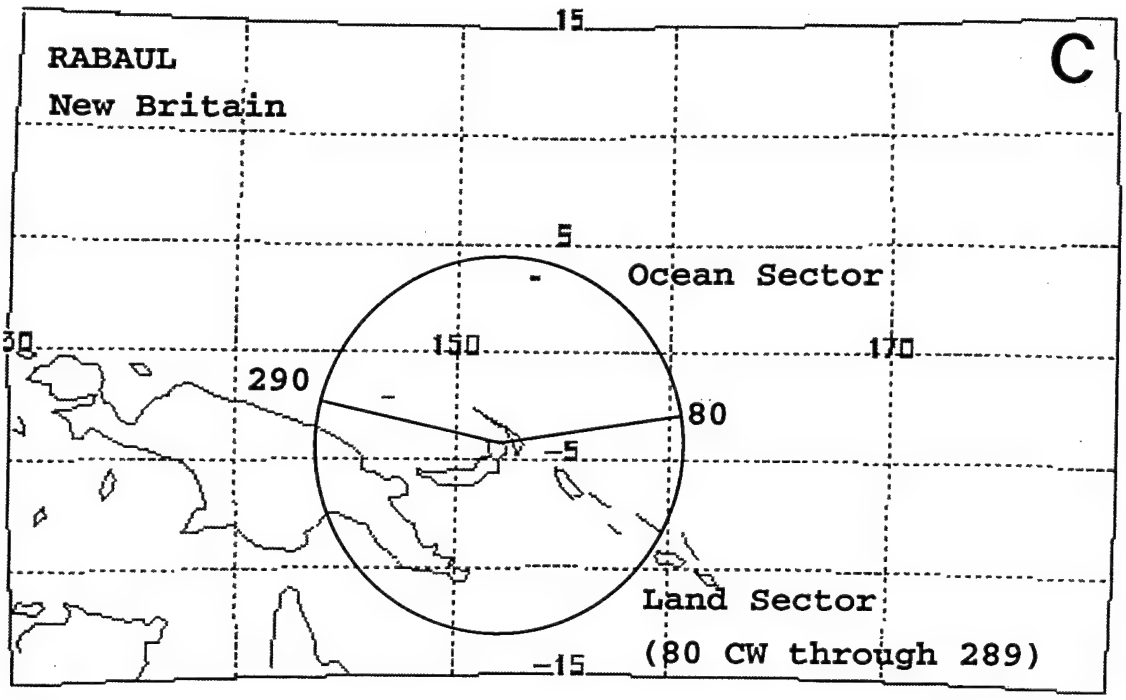

Fig. 3. (Continued)

Kavieng's sectors. Its land sector, 120° clockwise through 289°, includes many of the Solomon Islands, the Islands of New Ireland and New Britain as well as a large area of Papua New Guinea. Again, the rest of the area is considered to be ocean. Figure 3c shows how Rabaul's proximity to Kavieng dictated the choice of sectors. Rabaul's land sector includes the azimuth range 80° clockwise through 289°. As can be seen, both locales share many of the same land features in their land sectors.

Rabaul's ocean sector, unlike Kapingamarangi's or Kavieng's is somewhat "contaminated" by the large island of New Ireland (where Kavieng is located). The above land and ocean classifications are intended for use in the analysis of the characteristics of lightning activity as recorded be each DF (**CHAPTER IV**) as well as in the time series analysis portion of this study (**CHAPTER VI**).

The lightning data used in the thermodynamic section of this study are multi-DF lightning location data. In order to quantify whether any relationships exist between CAPE, CINE, θ_w and flash rates, smaller areas than those in Figs. 3a-c were chosen. In order to represent best any possible relationships, 7.2° x 7.2° latitude and longitude boxes centered around both Kavieng and Kapingamarangi were selected. The *XLIGHT* display software was then used to correctly de-limit the recorded lightning activity around each DF. Figure 4 shows the latitude and longitude boxes. In defining a parcel, the lowest 50 mb of the sounding are used when computing such parameters as CAPE, CINE, and θ_w. Throughout this investigation, these parameters refer strictly to the surface.

For both Kavieng and Kapingamarangi, flashes were summarized using the boxes shown in Fig. 4 during January and February of 1993. These two months were picked for several reasons. Traditionally, these months experience the strongest and best organized convective activity of the year due to the proximity of the TOGA-COARE region to the Australian summer monsoon regime (Chang and Krishnamurti 1987) Also, more thermodynamic data are available for these two months than for any other time period (four times daily in January and February versus twice daily otherwise). The 7.2° x 7.2° latitude/longitude boxes translate to a 800 km x 800 km area (6.4 x 10^5 km^2). This size was selected because it minimizes the possibility of erroneous intracloud and inverted waveform recordings while giving a good measure of the lightning activity in the vicinity of each DF. Lightning flashes are divided into ***"total-day"*** hourly flash rates, ***"individual-hour"*** flash rates, in addition to four, ***"six-hour"***

flash rate intervals that are comparable (in time) to the available thermodynamic data. The intent of the above techniques is to quantify whether a temporal or spatial link exists similar to that found in Darwin, Australia during the DUNDEE (Rutledge et al. 1992; Williams et al. 1992).

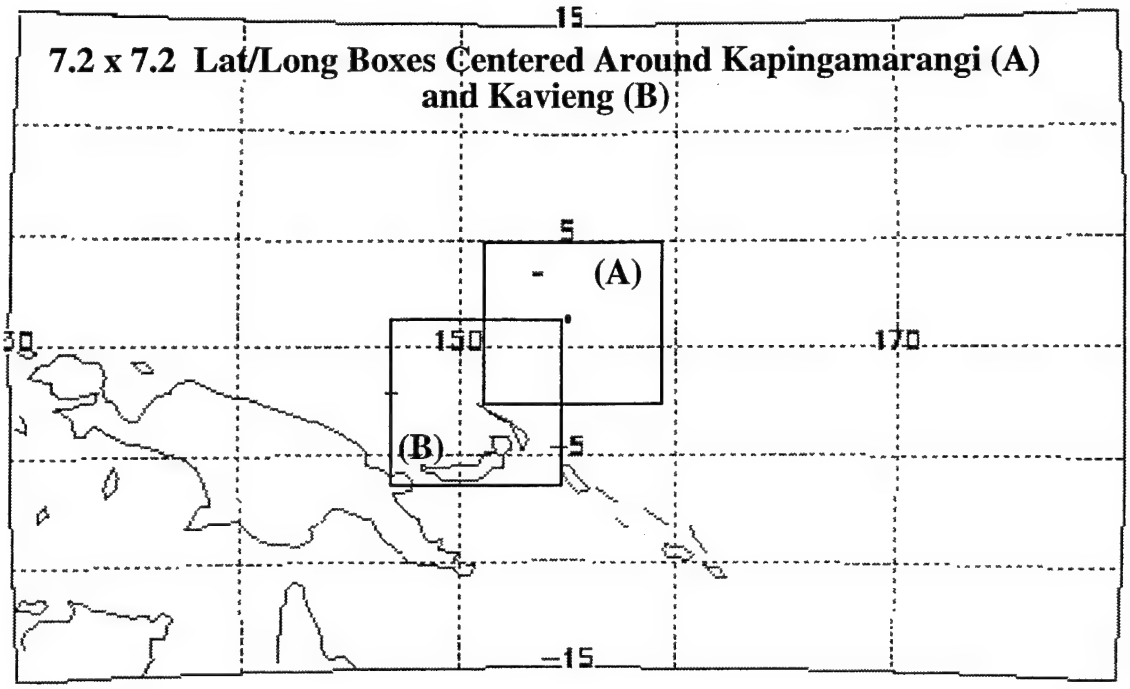

Fig. 4. Latitude/longitude boxes centered around Kavieng and Kapingamarangi used to de-limit lightning location data.

CHAPTER IV

1-DF ANALYSIS AND RESULTS

1. Basic Lightning Parameters

a) Land/ocean ratios

Daily flash total comparisons compiled by the Kapingamarangi, Rabaul and Kavieng DF's show that the Kavieng DF, on average, recorded much more lightning than Rabaul and Kapingamarangi. Closer examination of the data show that the Kavieng DF recorded higher flash counts 96.9% and 99.9% of the time compared to Kapingamarangi and Rabaul, respectively. Looked at from a totals point of view, the data show that the Kapingamarangi DF recorded 51% and 73% less flashes than Rabaul and Kavieng, respectively. It should be noted that the Kapingamarangi Atoll lies significantly away from any major land mass (~500 km) in contrast to the other two DF sites (see Fig. 3a). This implies that a good proportion of its convection is ocean spawned and one might, therefore, expect significantly less lightning to be recorded there, as is indeed the case (e.g., the experiments conducted by Takahashi 1978a,b at Ponape, Micronesia).

With few exceptions, land flashes were more prevalent than ocean flashes, especially during the months of January through April, and then again in November and December at all three locations. Table 1 shows a list of land/ocean ratios for all studied months as well as the percentage of time during which ocean flashes exceeded land flashes.

Table 1. Land/ocean ratios and percentage of time when ocean flashes exceed land flashes.

	Kapingamarangi		Rabaul		Kavieng	
Month	**L/O Ratio**	**Ocean flashes > land flashes**	**L/O Ratio**	**Ocean flashes > land flashes**	**L/O Ratio**	**Ocean flashes > land flashes**
Jan	7.4	0	14.2	0	11.2	0
Feb	3.4	0	6.3	0	10.1	0
Mar	2.4	14.3	7.0	0	6.0	3.2
Apr	2.5	3.3	6.8	0	7.5	0
May	1.1	35.4	3.0	3.3	3.2	22.6
Jun	0.8	78.5	2.0	2.0	4.6	3.3
Jul	0.6*	71.4*	1.1	48.4	3.1	12.9
Aug			0.7	64.5	0.9	48.4
Sep			0.9	73.3	1.7	43.3
Oct			1.9*	12.9*	3.4	14.3
Nov			4.8	0	3.9	6.9
Dec			8.1	0	7.6	0
Tot	**2.2**	**25.4**	**3.6**	**17.0**	**6.2**	**12.9**
Avg	**2.6**	**28.9**	**4.3**	**18.7**	**5.3**	**16.6**

***: DATA AVAILABLE FOR ONLY 14 DAYS**

Table 1 shows how at all three DF sites land/ocean ratios decrease from and average high of 11 in January to less than 1.0 (more ocean flashes) anywhere from June through September. This observation is noticed to be concurrent with an increase in the percentage of time (per month) when ocean flashes exceed land flashes. Since convective activity is at a minimum during the late northern hemisphere spring through early fall in this section of the equatorial tropics, the lack of obvious distinction between land and ocean flashes may be related to the convective minimum observed.

Closer analysis of the computed ratios reveal that the overall pattern observed in Table 1 does not match that obtained by Orville and Henderson (1986). Several factors contribute to this observation. For example, their study focuses on estimates

of global midnight lightning (i.e., a large spatial domain), and many climatic regimes within the same time period. In addition, while results from their study can be linked to features consistent with patterns of the general circulation of the planet, results from this study more closely highlight seasonality. The one feature that is nonetheless seen in both studies (through average values) is the overall predominance of lightning activity over the land versus the oceans.

Examining the total flash data from a radial perspective allows one to see the marked differences between the chosen land and ocean sectors. Total azimuthal distributions for all three DF sites are shown in Figure 5.

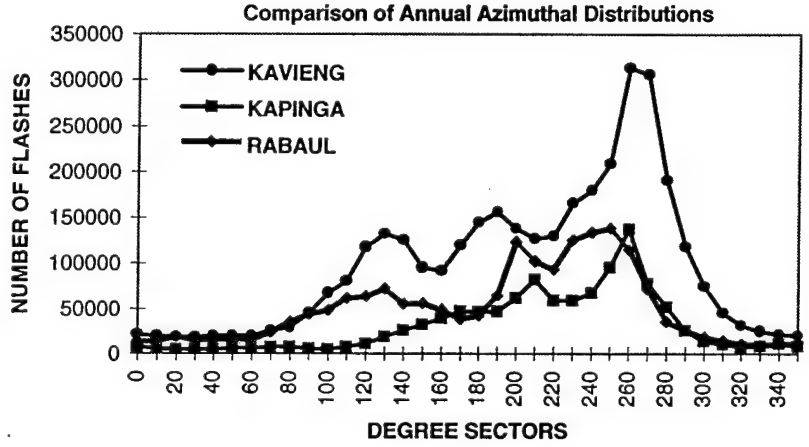

Fig. 5. Annual azimuthal distributions (per 10° sector) for all three DF's.

Note the particularly high totals obtained at all locations in the 200°-280° azimuth range. Within this range, over 50% of all recorded flashes are found. Specifically, this translates to 61% of Kapingamarangi flashes and 51% and 52% respectively, for Kavieng and Rabaul. The pervasiveness of lightning activity in these preferred

azimuths is most likely due to a combination of both land influences (through the stronger differential heating of the larger islands) and high sea surface temperatures.

Further analysis shows how Kapingamarangi's flash distribution is concentrated more along its land sector, while Rabaul's and Kavieng's, on the other hand, appear considerably broader. This is credited to the fact that Kavieng's and Rabaul's land sector lie further to the south. As a result, a larger area of ocean between the Solomon Islands and the eastern portion of Papua New Guinea is covered.

b) Percentage positive lightning

Statistics compiled on percentage positive lightning data show some interesting trends. Table 2 shows all the statistics grouped for total, land sector, and ocean sector flashes in a per month basis.

Table 2. Percentage of positive lightning statistics at all three sites for 1993.

	KAPINGAMARANGI			RABAUL			KAVIENG		
	Total	**Land**	**Ocean**	**Total**	**Land**	**Ocean**	**Total**	**Land**	**Ocean**
Jan	17.8	19.1	7.5	8.7	7.7	19.1	9.6	9.9	6.3
Feb	13.9	15.5	8.6	6.6	6.2	10.3	8.5	8.8	6.8
Mar	14.7	16.7	9.7	8.9	8.3	12.6	9.6	9.9	7.0
Apr	15.5	18.0	9.1	7.1	6.5	11.5	8.3	7.8	11.9
May	11.4	17.0	5.6	4.3	4.4	4.1	7.8	7.8	7.8
Jun	9.1	11.0	7.7	7.3	7.1	7.9	7.6	7.7	7.3
Jul	14.0	14.1	13.8	7.5	8.3	4.8	11.5	10.1	13.0
Aug				3.2	4.0	2.4	9.6	7.0	11.5
Sep				4.2	5.9	1.3	11.8	10.9	12.7
Oct				4.7	4.9	3.9	9.3	9.6	8.6
Nov				6.1	5.3	8.9	9.2	9.0	10.2
Dec				10.3	9.9	13.1	10.9	11.6	5.6
Avg	**13.8**	**15.9**	**8.9**	**6.6**	**6.5**	**8.3**	**9.5**	**9.2**	**9.1**
St. Dev	**2.8**	**2.7**	**2.6**	**2.2**	**1.8**	**5.3**	**1.4**	**1.41**	**2.67**

On all months available for comparison (January through July), note the relative dominance of positive flashes at Kapingamarangi versus Kavieng and Rabaul. The one exception is Kavieng's ocean flashes whose average value was the highest of the three. The higher frequency of positive flashes at Kapingamarangi may be attributable to the higher incidence of positive CG flashes often observed in the trailing stratiform region of convective systems (Engholm et al. 1990; Rutledge et al. 1990; Rutledge et al. 1992).

In Fig. 3a one can clearly see how the Kapingamarangi DF range encompasses a larger area of ocean than both Rabaul and Kavieng. Because of this, a greater percentage of the convection within the Kapingamarangi DF area is apt to be ocean generated while a smaller percentage of the activity likely moved from the land onto the ocean. Williams and Houze (1987) in a study of cloud clusters in the vicinity of Borneo (to the west of the TOGA-COARE region) find that cloud clusters over the oceans are considerably larger in area than those generated over land. These larger, prototypical sea clusters suggest that a significant stratiform component is found within them. Because of advection mechanisms within the stratiform region of a convective system, it is believed that the positive charge center is horizontally advected away (tilted dipole) from both the negative charge center and the area of strongest convection by the vertical wind shear. The result is an increase in positive CG flashes (Rutledge et al. 1990; Rutledge et al. 1992).

Others, however, suggest that the predominance of positive lightning away from the deepest convection is the results of in-situ charge separation mechanisms,

especially beyond 100 km. Although the horizontal advection theory is not abandoned, in situ processes better account for positive lightning in storms whose stratiform coverage away from the deepest convection greatly exceeds 100 km in length. Specifically, the increased incidence of positive lightning is related to charge separation by differential particle motions (i.e., ice to ice interactions) in the presence of supercooled liquid water (Engholm et al. 1990; Rutledge et al. 1990).

When comparing the findings of this study to similar research conducted within the United States, one finds significant differences. For example, Orville (1994) states that the annual percentage of positive lightning for the period 1989-1991 is 3.7%; ranging from 3.1% to 4.0%. Furthermore, he finds the percentages to be quite variable, in a geographical sense, with values as low as 2% around Florida and higher further north.

Although the aforementioned increase in areal coverage by the stratiform region of convective systems may still contribute to the higher frequency of positive flashes, the increase in the nominal range of each DF must also be considered. Brook et al. (1989) suggest that as long as a flash is within 600 km of a DF, the polarity of a flash may be recorded reliably. Since the gain of each TOGA-COARE DF was increased to approximately 900 km, an increase in the occurrence of positive flashes is not at all unexpected. It is stressed, however, that Brook et al.'s (1989) findings correspond to a limited number of winter storms studied over the United States. The effect of ionospheric reflections for storms strictly over the oceans (where attenuation is considerably weaker) and the whole issue of polarity reversal due to equipment sensitivity, has not been fully documented. The latter is especially so over the

equatorial tropics where a sparse number of lightning studies has been conducted. As is often the case, the reality of the increase in the percentage of positive lightning figures most likely lies somewhere between equipment sensitivity and nature.

c) Multiplicity

The multiplicity of a CG lightning flash is simply defined as the number of strokes in a flash. Monthly and annual statistics on positive and negative multiplicities show several interesting trends (see Table 3). For instance, positive multiplicity tallies indicate how there is little variability in these data as annual averages only range from 1.0 to 1.1 throughout the domain. This finding is not at all unexpected and agrees very well with Orville et al. (1987) who throughout the year observe 90% of positive lightning flashes with a multiplicity of one. The observation that positive multiplicities show little variation in space and time is consistent with the notion that positive CG flashes are composed (mainly) of a single stroke (leading to lower multiplicity values) and, followed by a period of continuing current (Uman 1987). Negative multiplicities, however, are, on average, higher in value ranging from 1.2 to 1.8. In addition to the higher average values, negative multiplicities also show more variability.

Seasonally, as well as spatially, several patterns (though admittedly weak) emerge. Notice how the lowest values at Kavieng and Rabaul tend to occur primarily during the months of July through October (the observed convective minimum) in both positive and negative multiplicities. The same cannot be said of the Kapingamarangi data (i.e., an obvious minimum), although this may be related to the limited amount of data available.

Table 3. Positive and negative multiplicity statistics at all three sites for 1993.

	KAPINGAMARANGI			RABAUL			KAVIENG		
	Total +/-	Land +/-	Ocean +/-	Total +/-	Land +/-	Ocean +/-	Total +/-	Land +/-	Ocean +/-
Jan	1.1/1.3	1.1/1.2	1.1/1.3	1/1.8	1/1.8	1.1/1.7	1.1/1.5	1.1/1.5	1.1/1.5
Feb	1.1/1.3	1.1/1.3	1.1/1.4	1.1/1.8	1.1/1.9	1.1/1.7	1.1/1.5	1.1/1.5	1.1/1.5
Mar	1.1/1.2	1.1/1.2	1.1/1.3	1.1/1.6	1.1/1.6	1.1/1.6	1.1/1.4	1.1/1.4	1.1/1.5
Apr	1.1/1.2	1.1/1.2	1.2/1.2	1.1/1.6	1/1.6	1.1/1.6	1.1/1.4	1.2/1.4	1.1/1.4
May	1.1/1.2	1.1/1.3	1.1/1.2	1/1.7	1/1.7	1/1.7	1.1/1.4	1.1/1.3	1.1/1.4
Jun	1.1/1.2	1.1/1.4	1/1.1	1/1.9	1/1.9	1/1.8	1.1/1.4	1.1/1.5	1/1.2
Jul	1.1/1.3	1.1/1.5	1/1.1	1/1.9	1/2.0	1/1.6	1.1/1.4	1.1/1.6	1/1.2
Aug				1/1.4	1/1.3	1/1.4	1.1/1.1	1.1/1.1	1/1.1
Sep				1/1.9	1/2.0	1/1.6	1.1/1.3	1.1/1.3	1/1.3
Oct				1/1.8	1/1.8	1/1.7	1/1.3	1.1/1.1	1/1.1
Nov				1/1.9	1/1.9	1/1.8	1/1.5	1.1/1.4	1/1.5
Dec				1/1.7	1/1.7	1/1.6	1/1.4	1.1/1.4	1/1.4
Avg	**1.1/1.2**	**1.1/1.3**	**1.1/1.2**	**1/1.8**	**1/1.8**	**1/1.6**	**1.1/1.4**	**1.1/1.4**	**1.0/1.3**
St. Dev	**0/0.1**	**0/0.1**	**0.1/0.1**	**.04/.2**	**.04/.2**	**.1/.1**	**.03/.14**	**.03/.15**	**.05/.16**

Spatially, Kapingamarangi's total, land and ocean positive multiplicities were highest, followed by Kavieng and Rabaul, respectively. For negative multiplicities (and for all flash designations) Rabaul's annual averages were highest followed by Kavieng and Kapingamarangi. Observe, too, the fact that the negative multiplicity high-to-low distribution is seen to occur during 100% of monthly values in addition to annual averages.

The distribution of lightning activity per multiplicity increment (total multiplicity) shows the obvious dominance of low multiplicity flashes within this region of the equatorial tropics. At all three sites, over 82% of flashes recorded were of multiplicity one or two. Although monthly numbers vary slightly, this general dominance is seen throughout the year. Figures 6a-c shows histograms for all three flash categories.

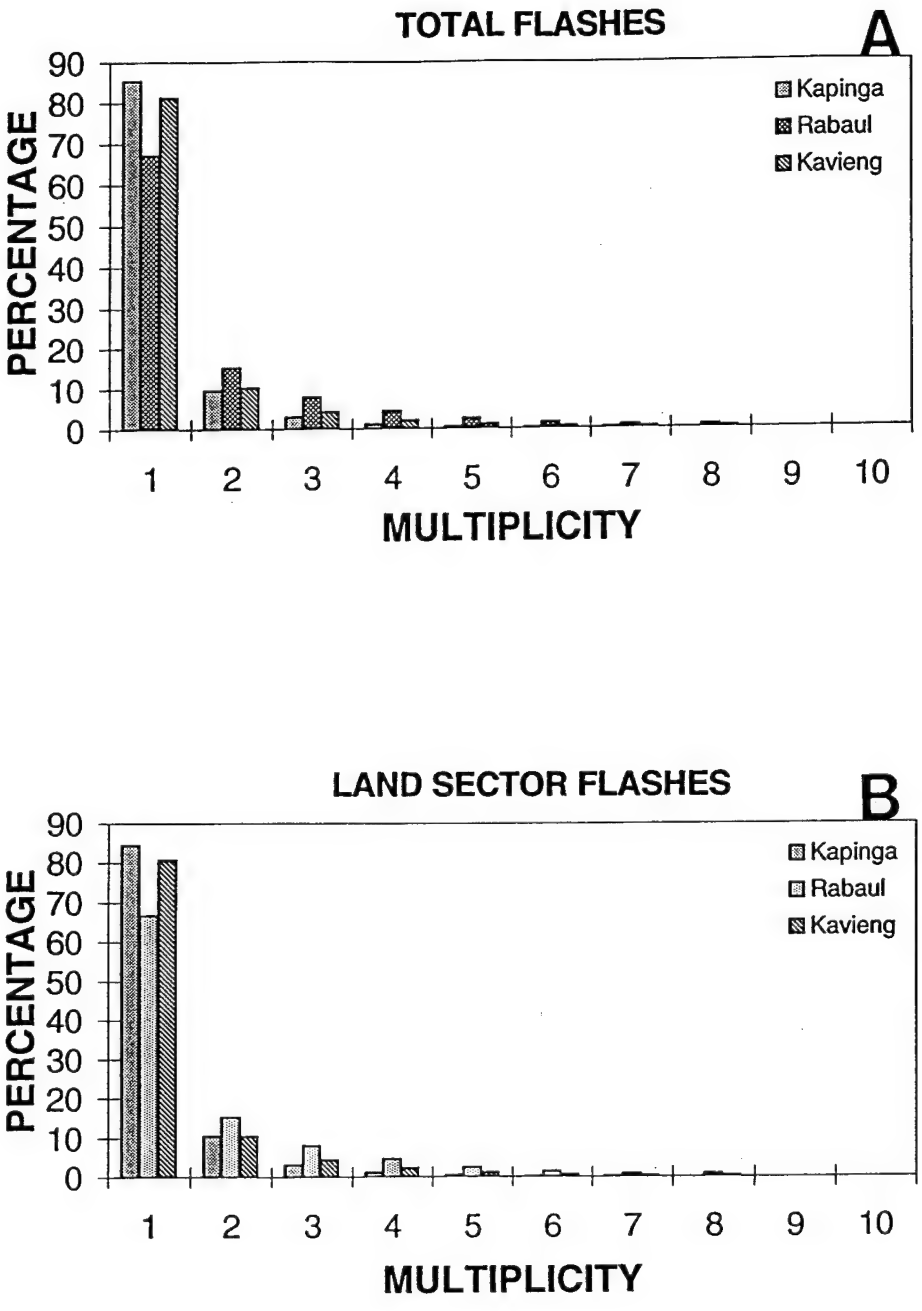

Fig. 6. Comparison of multiplicity versus percentage of occurrence for total (a), land (b), and ocean (c) flashes.

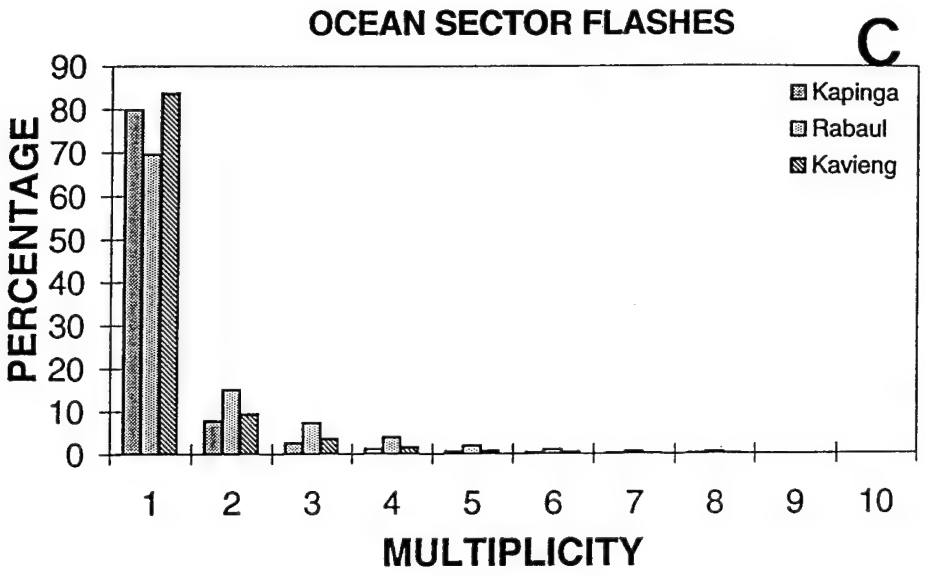

Fig. 6. (Continued)

The observed stability of single stroke flashes in the TOGA-COARE region (positive and negative combined) is in sharp contrast to CONUS results, for example, compiled by Orville et al. (1987) and Reap and MacGorman (1989). They show how single stroke flash percentages vary significantly throughout the year.

2. Diurnal Variation of Lightning

The diurnal variation of lightning activity has long been the subject of intensive research, especially over the continental United States (e.g., Lopez and Holle 1986; Reap 1986). The study of convection patterns (through the use of satellite data) has been studied by Williams and Houze 1987 and Mapes and Houze 1993 in and around the maritime continent (warm pool region). In this study, diurnal cycles of lightning are studied strictly from the land and ocean sector perspectives. Histograms of lightning activity are plotted as functions of average flashes per hour versus local standard time (LST). For each location the data were studied for the entire period as well as for three month time intervals in order to assess any possible seasonality. Flashes were averaged per hour for every period in order to smooth each hourly segment and therefore prevent the overinfluence of any one interval. Results from this portion of the study are compared to satellite-derived studies of convection in and around the warm pool region and to selected midlatitude (CONUS) studies of lightning activity.

Figures 7 and 8 show graphs for the total time period for land and ocean flashes, respectively, while Table 4 summarizes the characteristics of the chosen temporal break-ups. Observe in Fig. 7 the broad maximum which is seen to occur between 2100 and 0500 LST. Of special interest, too, is the fact that Rabaul's graph shows a secondary maximum at 1400 LST, while Kavieng's data displays a broad, but marked early afternoon to early evening increase in lightning activity. Minimums in activity occur between 0900 and 1200 LST with a persistent and sharp drop-off in activity that

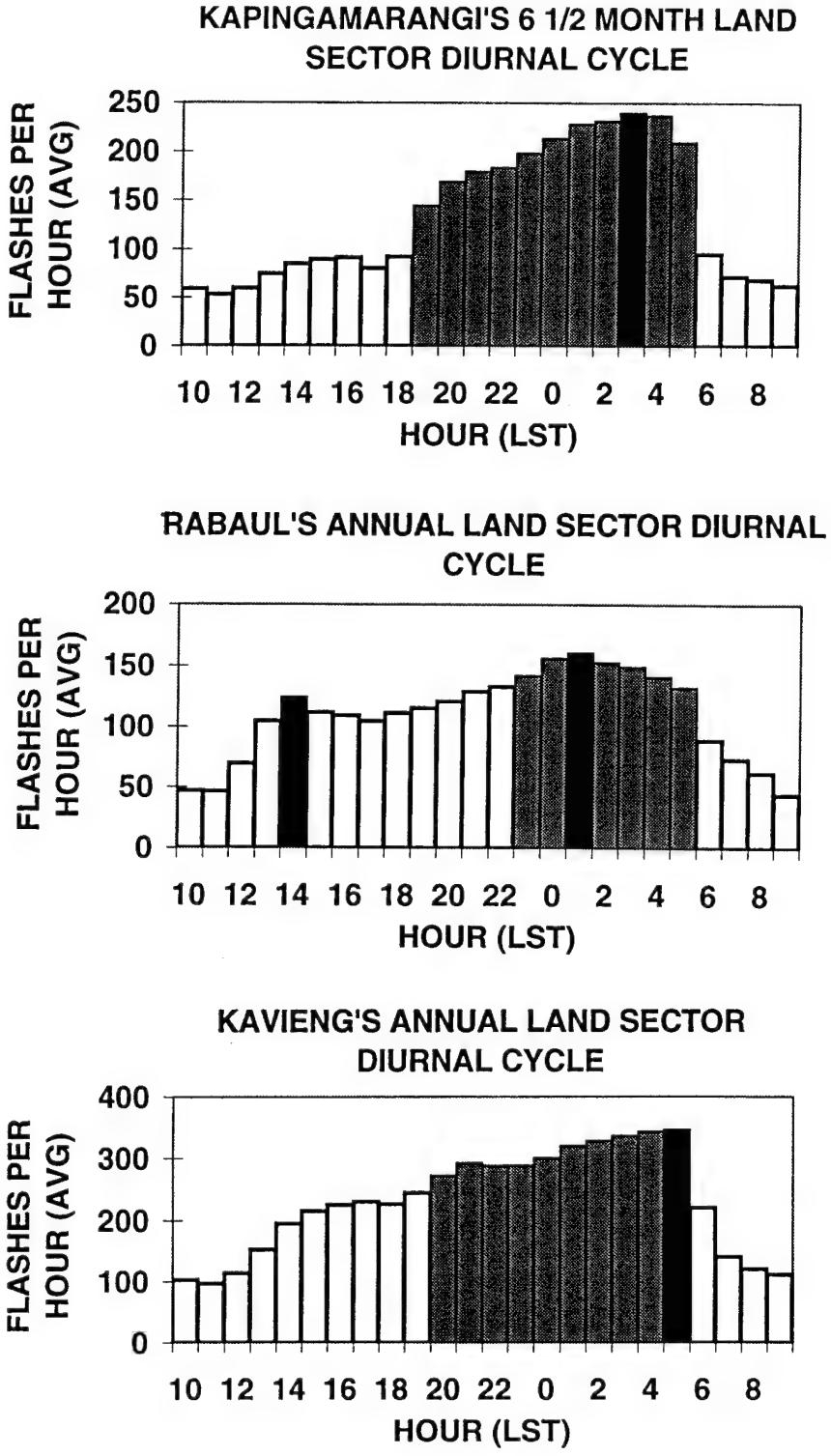

Fig. 7. Annual and 6 1/2 month land sector diurnal variations of lightning for all three DF sites. Gray shading indicates broad maximum in lightning activity, and black indicates an observed peak.

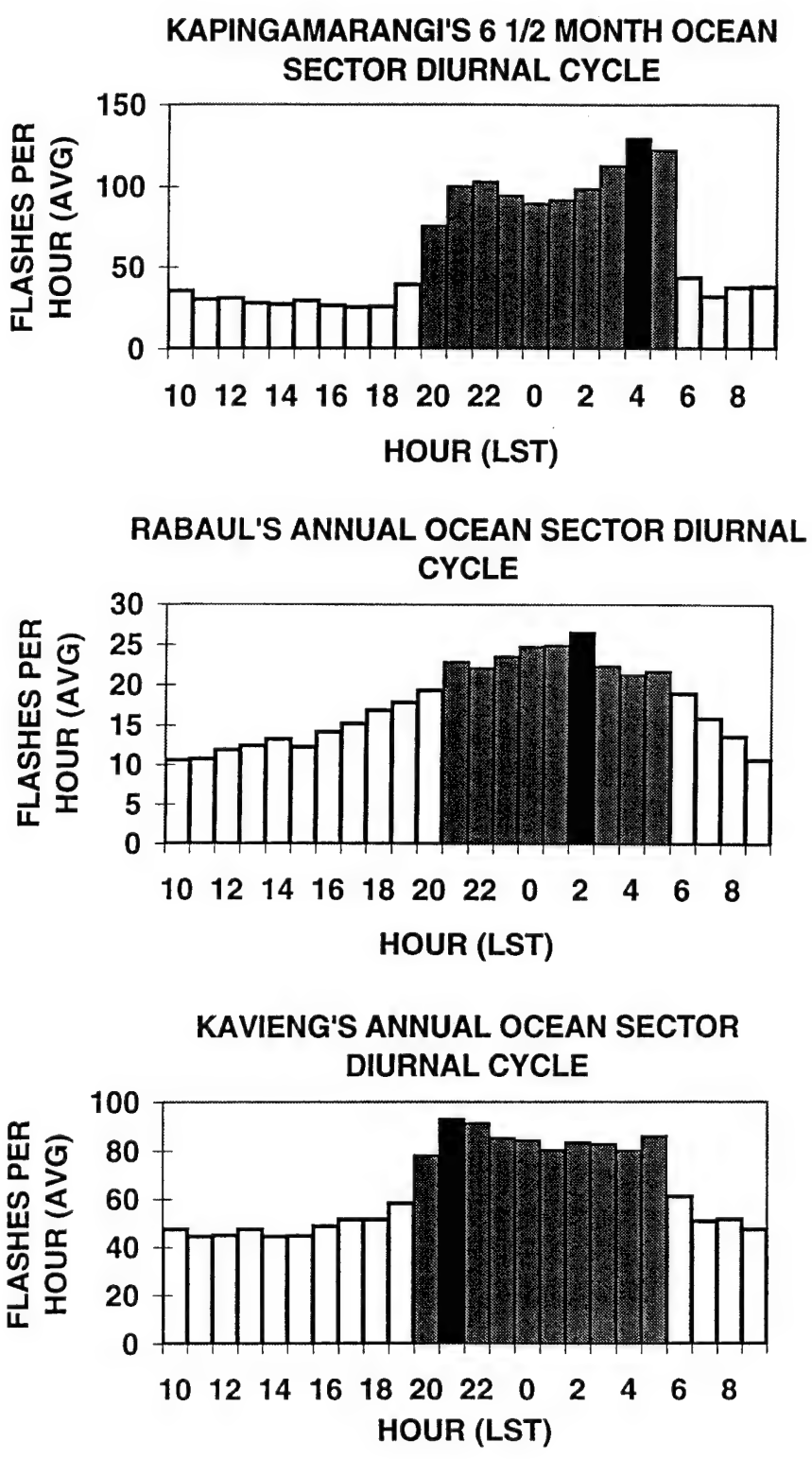

Fig. 8. Annual and 6 1/2 month ocean sector diurnal variations of lightning for all three DF sites. Gray shading indicates broad maximum in lightning activity, and black indicates an observed peak.

Table 4. Monthly interval diurnal variations in lightning activity. Ranges in maximums and minimums are shown as well as peaks and absolute minimums. All times are LST.

	Minimums			Maximums		
	Jan-Apr	**May-Aug ***	**Sep-Dec**	**Jan-Apr**	**May-Aug ***	**Sep-Dec**
Kapinga* (Land)	1000-1200 Min: 1100	1000-1600 Min: 1200	N/A	2300-0500 Peak: 0300	0000-0300 Peak: 0400	N/A
Kapinga* (Ocean)	1000-1600 Min: 1300	1500-1800 Min: 1700	N/A	2100-0500 Peak: 0400	2100-0500 Peak: 0400	N/A
Rabaul (Land)	0900-1100 Min: 1100	0900-1000 Min: 1000	0900-1100 Min: 1100	2300-0500# Peak: 0100	2100-0500# Peak: 0100	2 peaks: 1400/0000
Rabaul (Ocean)	0900-1100 Min: 1100	1500-1700 Min: 1500	0900-1000 Min: 0900	2300-0600 Peak: 0200	2100-0500 Peak: 0500	2100-0400 Peak: 2100
Kavieng (Land)	1000-1200 Min: 1100	1000-1300 Min: 1200	1000-1300 Min: 1200	0000-0500@ Peak: 0300	2100-0500@ Peak: 0500	2100-0500@ Peak: 0500
Kavieng (Ocean)	1100	1200-1800 Min: 1400	0900-1500 Min: 1100	2100-0300 Peak: 0100	2100-0500 Peak: 0500	2000-0500 Peak: 2100

***: Calculated for May-Jul 14th; #: Secondary peaks at between 1300 and 1400; @: Broad increase in lightning activity though the late afternoon hours (no secondary peaks)**

always occurs between 0500 and 0600 LST. Figure 8 (the ocean sector activity) shows a similar, but again clearly broad, maximum between 2000 and 0500 LST with two observed peaks at each location. No late morning or early afternoon peaks are apparent, and minimums in activity are considerably broader ranging from approximately 0800 to 1500 LST (through to 1800 LST at Kapingamarangi, though). Consistent with the land sector results is the same sharp drop-off in lightning activity that occurs between 0500 and 0600 LST.

Table 4 summarizes seasonal time intervals for both land and ocean sectors. The table serves to highlight the similarities in the times of maximum and minimum activity in time and space, with ***few*** exceptions. This overall pattern agrees favorably with the consensus that convective activity over this part of the equatorial tropics experiences a

nighttime maximum (Williams and Houze 1987; Mapes and Houze 1993). This is evident through both annual and monthly time interval statistics (Figs. 7, 8 and Table 4).

A more cursory examination of the data shows how remarkably different the diurnal behavior of lightning activity is when compared to that of a typical continental United States location. Studies of lightning in eastern Colorado, central Florida (Lopez and Holle 1986), and throughout the western United States (Reap 1986) clearly point to a favored time interval during which lightning activity peaks. This interval, on average, ranges from 1500 to 1800 LST with a near zero minimum in the early morning hours. The above figures and table clearly indicate that lightning activity, in the overall sense, never drops to near zero; a fact also evident in individual monthly data (not shown here). Instead, the pattern shows a sharp drop off in the average hourly number of flashes after 0500 LST, followed by a somewhat leveled pattern of activity during the late morning and early afternoon. This is in sharp contrast to the Colorado and Florida data which display a gradual decrease in activity soon after peak time. Furthermore, Lopez and Holle (1986) allude to a remarkably large degree of variability in the day-to-day diurnal progression of lightning. This, again, is in stark contrast to the TOGA-COARE results which show a more notably stable pattern from day-to-day.

The marked differences between the diurnal cycles found within the TOGA-COARE region and that of a typical continental United States location point to the fact that convection over the western Pacific Ocean is not strictly driven by the diurnal

cycle of heating (as are many areas within the United States). Noteworthy is the fact that Rabaul's land cycles (all periods) show persistent secondary peaks between 1300-1400 LST while Kavieng's land cycles (again, all periods) show broad increases in flashes beginning in the early afternoon. This phenomenon is likely due to thunderstorm activity forming over Papua New Guinea, New Britain, and New Ireland where stronger differential heating occurs. The observance of secondary peaks and broad increases in lightning activity are the only hints that suggest that differential heating may be playing a role in the diurnal cycle of lightning in the TOGA-COARE region. This is a fact which is neatly accentuated by the Kapingamarangi land sector. Note how Kapingamarangi's data (whose land sector does not encompass ***any*** portion of Papua New Guinea) do not show either a late afternoon peak nor a significantly broad increase in flash activity beginning in the early afternoon and continuing through the late afternoon.

The observed land and ocean variations agree very well with previous research on satellite-derived cloud cluster climatologies and the notion that these features undergo a diurnal cycle as well. Cloud clusters, or connected areas of cloudiness with blackbody temperatures below a certain threshold, can be objectively tracked and categorized into land and ocean regimes (Williams and Houze 1987). They show, in the vicinity of Borneo (west of the TOGA-COARE region), how large cloud clusters (area $> 1.2 \times 10^5$ km^2) tended to develop over the oceans in the early morning hours while no clusters which met the above criterion developed over the land.

In an expansion of the Williams and Houze (1987) study, Mapes and Houze (1993) show how very cold cloudiness (i.e., deep convection with cloud tops < 208K or -65°C) peaks before dawn and diminishes throughout the morning. This fact matches the observed diurnal variation in lightning activity, which, as a whole, reaches a maximum in the early morning hours (0000-0500 LST). In addition, they find that a smaller scale diurnal cycle is present in which a "burst" of small cloud clusters appear over the larger islands (Indonesia region) in the afternoon. These smaller cloud clusters are lower in height and are termed moderately cold cloudiness (i.e., cloud top temperatures <233K or -40°C). Of interest, though, is the fact that the afternoon burst is seen to be pseudo-coincident with the previously mentioned secondary peaks and broad afternoon increases in lightning at Rabaul and Kavieng, respectively.

CHAPTER V

THERMODYNAMICS AND LIGHTNING ACTIVITY

1. Distribution of Thermodynamic Variables

As seen in chapter IV of this study, the distribution of lightning activity is remarkably biased towards land masses (i.e., the larger islands and adjacent warm waters). This bias is noticed, as well, in time, as evident in the diurnal variations of lightning activity. The aims of this chapter are to show the temporal and spatial variations of CAPE, and θ_w throughout the TOGA-COARE region (as shown in Fig. 2). In addition, several analyses of hourly flash rates of lightning against the above variables are presented in an effort to quantify what, if any relationships, exist between them.

Williams and Renno (1993) have shown that there is a "...reasonably well-defined..." linear relationship between CAPE and the θ_w of the boundary-layer pointing to the θ_w distribution as a good indicator of the available energy stored within the tropical atmosphere. Global climatologies of mean maximum θ_w's for January and July indicate that values for the entire TOGA-COARE range between 23°C and 25°C. The following tables (Tables 5 - 7) present a picture of the spatial and temporal distributions of CAPE, and θ_w as well as a summary of how linearly correlated CAPE, and θ_w were observed to be. Monthly, and time interval averages are shown for all four locations (except for the CAPE/θ_w R^2 and R table) in order to show the variations of each parameter through the OSA.

Table 5. Temporal and spatial distributions of θ_w. Temperatures are in °C.

KAVIENG	0500 UTC	1100 UTC	1700 UTC	2300 UTC	Monthly Average
Jan	24	24	24	23.7	23.9
Feb	24.1	24.3	24.6	24.1	24.3
TIME AVERAGE	***24.1***	***24.2***	***24.3***	***23.9***	
TOTAL AVERAGE	***24.1***				
KAPINGAMARANGI					
Jan	22.7	23	22.6	22.5	22.7
Feb	22.9	23.2	23.1	23	23
Mar		23.3		23.2	23.3
Apr		23.8		23.9	23.9
May		24		24.2	24.1
Jun		23.8		23.6	24.1
TIME AVERAGE	***22.8***	***23.5***	***22.9***	***23.4***	
TOTAL AVERAGE	***23.5***				
NAURU					
Jan	23.6	23.8	23.5	23.1	23.6
Feb	23.3	23.2	23.1	22.9	23.5
Mar		23.2		23.2	23.2
Apr		23.5		23.5	23.5
May		23.3		23.6	23.5
Jun		23.3		23.4	23.4
TIME AVERAGE	***23.5***	***23.4***	***23.3***	***23.3***	
TOTAL AVERAGE	***23.5***				
MANUS					
Jan	23.2	23.3	23.4	23.1	23.3
Feb	23	23.3	23.2	22.9	23.1
Mar		22.9		22.8	22.9
Apr		23.4		23	23.2
May		23.7		23.5	23.6
Jun		24		23.7	23.9
TIME AVERAGE	***23.1***	***23.4***	***23.3***	***23.2***	
TOTAL AVERAGE	***23.3***				

Table 6. Temporal and spatial distributions of CAPE (in J Kg^{-1}).

KAVIENG	0500 UTC	1100 UTC	1700 UTC	2300 UTC	Monthly Average
Jan	817	1037	1109	615	895
Feb	1150	1589	2064	1289	1523
TIME AVERAGE	***1392***	***1313***	***1587***	***952***	
TOTAL AVERAGE	***1209***				
KAPINGAMARANGI					
Jan	101	221	199	132	163
Feb	302	492	534	383	427
Mar		643		434	539
Apr		790		801	796
May		982		998	990
Jun		774		538	656
TIME AVERAGE	***202***	***650***	***367***	***548***	
TOTAL AVERAGE	***595***				
NAURU					
Jan	593	808	612	310	581
Feb	400	429	445	186	365
Mar		486		353	420
Apr		447		283	365
May		449		384	417
Jun		281		226	254
TIME AVERAGE	***497***	***483***	***529***	***290***	
TOTAL AVERAGE	***400***				
MANUS					
Jan	229	432	580	311	388
Feb	282	603	620	307	453
Mar		354		237	296
Apr		445		204	325
May		664		430	547
Jun		909		725	817
TIME AVERAGE	***256***	***568***	***600***	***369***	
TOTAL AVERAGE	***471***				

Table 7. Temporal and spatial distributions of CAPE/ θ_w R^2 values and correlation coefficients, R (in parenthesis).

KAVIENG	0500 UTC	1100 UTC	1700 UTC	2300 UTC
Jan	0.82	0.67	0.75	0.75
	(0.90)	(0.82)	(0.87)	(.087)
Feb	0.91	0.94	0.92	0.96
	(0.95)	(0.97)	(0.96)	(0.98)
R^2 Range: 0.67-0.96				
R Range: 0.82-0.98				
KAPINGAMARANGI				
Jan	0.49	0.34	0.51	0.52
	(0.70)	(0.58)	(0.71)	(0.72)
Feb	0.64	0.79	0.79	0.68
	(0.80)	(0.89)	(0.89)	(0.82)
Mar		0.78		0.71
		(0.88)		(0.84)
Apr		0.91		0.79
		(0.95)		(0.89)
May		0.88		0.91
		(0.94)		(0.95)
Jun		0.65		0.71
		(0.80)		(0.84)
R^2 Range: 0.34-0.91				
R Range: 0.58-0.95				
NAURU				
Jan	0.80	0.90	0.87	0.77
	(0.89)	(0.95)	(0.93)	(0.87)
Feb	0.76	0.80	0.73	0.68
	(0.87)	(0.89)	(0.85)	(0.82)
Mar		0.75		0.70
		(0.86)		(0.84)
Apr		0.58		0.64
		(0.76)		(0.80)
May		0.68		0.59
		(0.82)		(0.77)
Jun		0.71		0.60
		(0.84)		(0.77)
R^2 Range: 0.59-0.90				
R Range: 0.77-0.95				

Table 7. (Continued)

MANUS				
Jan	0.50	0.60	0.73	0.65
	(0.71)	(0.77)	(0.85)	(0.81)
Feb	0.80	0.77	0.76	0.75
	(0.89)	(0.87)	(0.87)	(0.87)
Mar		0.58		0.73
		(0.76)		(0.85)
Apr		0.70		0.60
		(0.84)		(0.77)
May		0.87		0.85
		(0.93)		(0.92)
Jun		0.73		0.87
		(0.85)		(0.93)
R^2 Range: 0.50-0.87				
R Range: 0.71-0.93				

NOTE: Before any analysis results are given, it is once again, reiterated, how these data are preliminary in nature. Therefore, any results are to be considered preliminary as well.

The distribution of θ_w through the OSA shows that the highest average θ_w values occur at Kavieng (all months and times) followed by Nauru, Manus Is., and Kapingamarangi (Table 5). This distribution pattern agrees well with global climatologies of θ_w which show elevated values (i.e., well-defined maxima) near to land masses with decreasing values away from land. This distribution stems from the difference in temperature between the ocean and the land created by a sharp differential of heating heating between the two surfaces (Williams and Renno 1993).

Table 6, on the other hand, shows the distribution of CAPE. Once again, Kavieng's average values are highest (all times and dates) and by at least a factor of two. The times with the lowest average CAPE values are always 2300 and 0500 UTC (0900 and 1500 LST) for all locations via examination of January and February data. This 0900 to 1500 LST time interval is the typical period during the day when convection, and lightning activity, are at a minimum. In looking at the diurnal variation of CAPE at Darwin, Australia, Williams and Renno (1993) show how CAPE is essentially sustained throughout the course of the day. Although the 0900 to 1500 LST is evident in the average values, it is now stressed how daily CAPE's do indeed show a high degree of sustainability from day-to-day in the TOGA-COARE region.

Examination of the previously mentioned, and well-defined CAPE/θ_w linear relationship using the TOGA-COARE sounding data, reveal no surprising results (see Table 7). Williams and Renno (1993) show that CAPE is seen to increase approximately linearly with θ_w with correlation coefficients of 0.8 to 0.9. This stems from the fact that tropical soundings remain largely invariable through most of the troposphere except for changes in the boundary-layer environment. Table 7 indicates that the Kavieng sounding data displays the "best" linear relationship of all four locations with correlation coefficients ranging from 0.82 to 0.98. The value of θ_w for which CAPE is essentially zero is consistently around 23°C. Data from the other stations show good correlations and the same zero-CAPE/θ_w relationship. The observed "deterioration" in the R^2 and R values, however, may be credited to the inherent errors within the data.

In spite of the seemingly well-behaved patterns observed in the data shown in Tables 5-7, the corrupted state of some of the data do show. It is stressed that, more than likely, only Kavieng's data appear reliably accurate. This is based, solely, on comparison of the results with data gathered by previous research, and, of course, prior knowledge of sounder malfunctions.

The somewhat reliable nature of Kavieng's data set is evident in all three previous tables. Not only are Kavieng's θ_w values within a degree of those computed for climatologies (Williams and Renno 1993), but CAPE values appear as "high" as would be expected for a typical tropical sounding. Neglecting, for the moment, any barriers to convection or possible differences in CAPE due to the computation procedure chosen, data collected at truly maritime locales show how CAPE values should indeed be high (i.e., > 1000 J Kg^{-1}) regardless of the proximity of the station to any significantly large land mass. Observations from the GATE experiment (Lucas et al. 1994a using corrected values from Zipser and LeMone 1980) show that CAPE's average around 1500 J Kg^{-1} which is fairly comparable to the values observed at Kavieng. The dramatic difference in CAPE's between Kavieng and the other three stations is thus attributed to equipment malfunctions and not to nature. One final fact that attests to the robustness of Kavieng's data (relative to the other sites, at least) is the "better" linear relationship observed between its CAPE and θ_w values (see Table 7).

2. Thermodynamic Variables Versus Lightning Flash Rates

a) Background

This section focuses on various analyses of lightning flash rates versus CAPE and θ_w. The former is conducted to see if a spatial or temporal link exists akin to that found by Rutledge et al. (1992) and Williams et al. (1992) during the DUNDEE in Darwin, Australia. Here, some of the same methodology employed by the previous authors is used, with the exception of the monsoon versus break period classification.

Graphically, CAPE is the "positive" area on a thermodynamic diagram enclosed by the temperatures profiles of the environment and of the lifted parcel. By convention, this area is defined as the theoretical maximum energy available to an upwardly displaced parcel of air above its level of free convection (LFC) and below the level of neutral buoyancy (LNB). CINE, on the other hand, is taken to be, again by convention, as the negative area (below the LFC) that essentially serves as a barrier to convection. In other words, it is the energy against which the environment has to work in order for a parcel to achieve its convective potential (or CAPE; Emanuel 1994).

As stated in CHAPTER IV, the lightning data were space delimited to 400 km x 400 km lat/long boxes around both Kavieng and Kapingamarangi, the only sites with collocated sounder locations and DF's. The underlying assumption here is that CAPE is a good measure of the potential vigor of convective activity. The remainder of this chapter explores the possible CAPE/θ_w flash rate relationship.

b) CAPE and θ_w versus flash rates

Figure 9 shows the CAPE versus flash rate activity (for Kavieng) three different ways. Fig. 9a shows the daily flash rate versus daily average CAPE, while Fig. 9b represents the maximum daily flash rate versus the CAPE time period chosen as representative of the preconvective environment for both Kapingamarangi and Kavieng. The CAPE time period chosen and used throughout this study is 0500 UTC or 1500 LST. The basis for this selection is that this is the time of the day prior to the onset of the most vigorous convection (Mapes and Houze 1993) and lightning activity (as seen in CHAPTER IV of this investigation). Finally, Fig. 9c shows hourly CAPE versus temporal flash rates on either side of the CAPE. Note, essentially, the true and virtually categorical lack of correlation in all the figures. In Table 8 notice how exceedingly low the R^2 values are. Assuming an independent, normal distribution for each pair of 59 observations, and testing the null hypothesis that $R^2>0$ at the 90% confidence level, shows that even the highest R^2 of 0.14 has no real significance. The results vary very little from Kapingamarangi to Kavieng in spite of the assumed differences in data quality.

Although CAPE represents the potential available buoyant energy within a given environment, the question of why oceanic clouds achieve such a small portion of this energy remains. Zipser and LeMone (1980) and Lucas et al. (1994b) have shown remarkable differences in the vertical velocities of rising parcels between continental and oceanic clouds, respectively. While work from DUNDEE suggests a robust

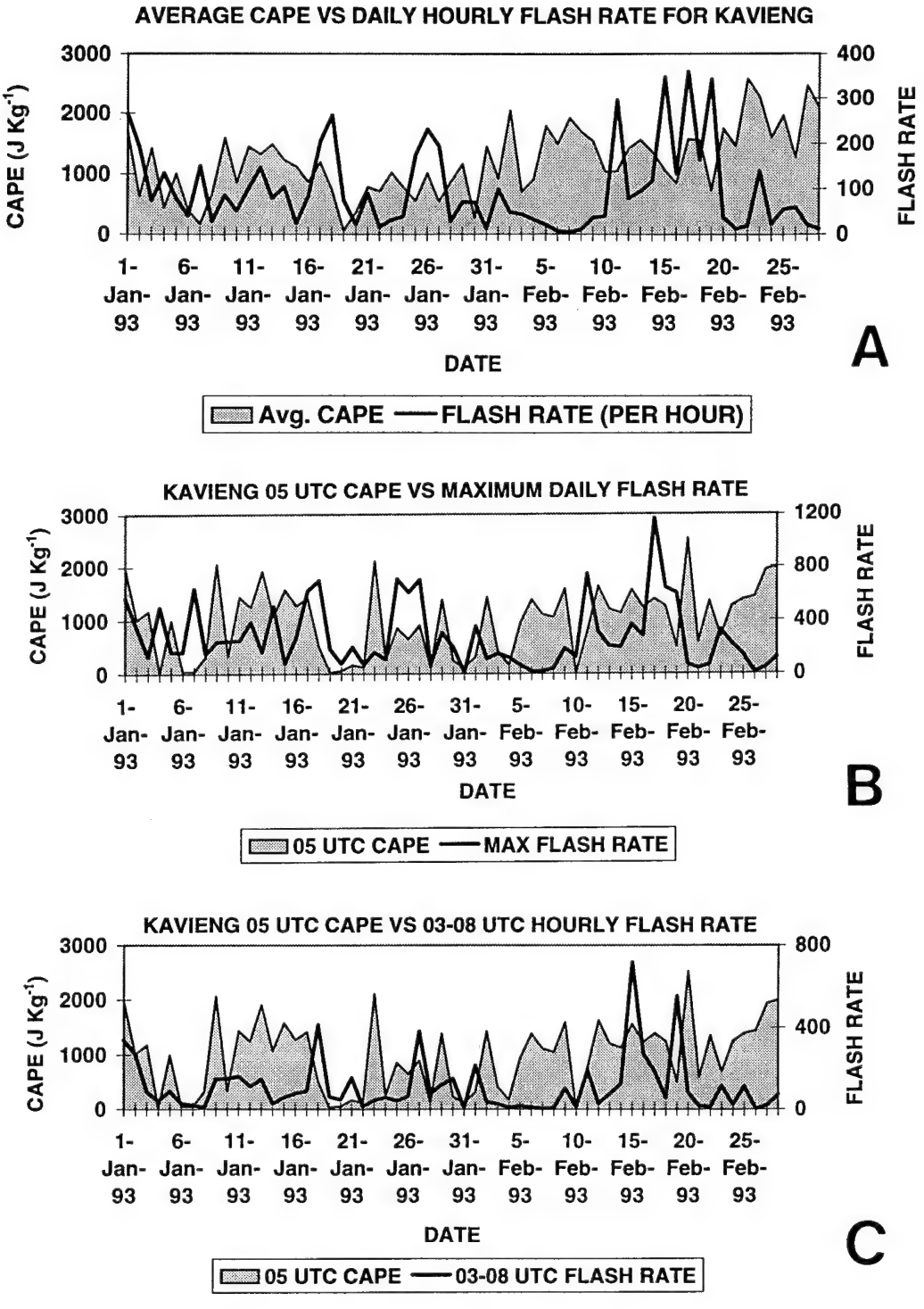

Fig. 9. Daily flash rate versus average CAPE (a), maximum daily flash rate versus CAPE for representative time period (0500 UTC/1500 LST; b), and hourly CAPE against time interval flash rate for Kavieng.

CAPE/flash rate relationship, its ideal location, with distinctively different source regions, facilitated the continental versus maritime classification. Within the TOGA-COARE region, flow regimes do vary, but the air has a sufficiently long residence time over the ocean surface to make a such as classification attempt not as satisfying.

Table 8. CAPE versus flash rate R^2 values for Kavieng and Kapingamarangi.

CAPE VS. FLASH RATE		
	R^2's	
	KAVIENG	KAPINGA
AVG CAPE VS. DAILY FLASH RATE	0.03	0.13
05 UTC CAPE VS. MAXIMUM DAILY FLASH RATE	0.0004	0.009
05 UTC CAPE VS 03-08 UTC FLASH RATE	0.01	0.14
11 UTC CAPE VS 09-14 UTC FLASH RATE	0.001	0.10
17 UTC CAPE VS 15-20 UTC FLASH RATE	0.05	0.04
23 UTC CAPE VS 21-02 UTC FLASH RATE	0.04	0.08

The distribution of CINE at Kavieng and Kapingamarangi shows that values range from zero to 190 J Kg^{-1} (mean of 35 J Kg^{-1}) and from zero to 350 J Kg^{-1} (Mean of 98 J Kg^{-1}), respectively. The seemingly high values at Kapingamarangi are attributed to data limitations, while those of Kavieng resemble results gathered at DUNDEE (Williams and Renno 1993). Table 9 shows the individual temporal breakups and the theoretical updraft speed required to reach the positive energy area and achieve the parcel's convective potential.

Table 9. Temporal distribution of CINE (J Kg^{-1}), updraft speed (in m s^{-1}, and in parenthesis) required to breakthrough CINE at Kavieng and Kapingamarangi.

	05 UTC	11 UTC	17 UTC	23 UTC	TOTAL
Kapinga	99 (14.1)	99 (14.1)	93 (13.6)	101 (14.2)	98 (14)
Kavieng	37 (8.6)	41 (9.1)	28 (7.5)	34 (8.2)	35 (8.3)

Although the CINE values are comparatively small, they "...are by no means negligible" Williams and Renno (1993). The figures on Table 9, particularly Kavieng's, agree very well with Williams and Renno (1993) who show CINE values that range between zero and 200 J Kg^{-1} throughout several tropical locations. Others, however (Alexander and Young 1992; Griffith and Zipser 1993) have shown that CINE values can be much lower than those computed in this study (~5 J Kg^{-1}) and with a smaller range. In spite of the observed differences, these figures strongly suggest that CINE is indeed a significant barrier to the release of conditional instability within the tropical atmosphere. A good correlation between ***high*** flash rates and ***low*** CINE or vice versa was not observed. This points to the availability of other barriers that may be present, and most likely interacting with one another.

The issue of weakly electrified oceanic storms is a subtle one. Most likely, the answer lies amidst several factors. With a greater coverage of convection over the oceans (especially at night), more mesoscale downdrafts exist, and, in turn, more significant water loading of potential air parcels results. The effect of this increase in water loading is a reduction in the low-level buoyancy of parcels, essentially limiting the strength of updrafts and strengthening the presumed cap to vigorous convection. A direct result of weaker updrafts (as researched by Jorgensen and LeMone 1989 and

Lucas et al. 1994b) is a reduction in the amount of liquid condensate available in the mixed-phase region of a cloud *($0°C \leq T \leq -40°C$)*.

Research by Takahashi (1978), Rutledge et al. (1992), and Williams et al. (1992) shows that most of the precipitation that forms from oceanic cloud systems is a "warm rain" coalescence process. Also, Gamache (1990) states that most of the condensate that does make it above the freezing level is predominately in the ice phase. Results from all these works agree very well with each other and confirm the idea of less liquid condensate in the mixed-phase region of clouds. The importance of the above facts are examined in greater detail by Williams et al. (1991), and Dong and Hallett (1992) who show how crucial mixed-phase microphysics are in charge separation processes that lead to cloud electrification. These are processes, the authors insist, that are strongly dependent on cloud temperature and liquid water content.

The possible θ_w/flash rate relationship was also observed to be equally weak. As in the CAPE/flash rate regressions, the data were found to be uncorrelated (see Table 10). This lack of correlation, however, is not at all unexpected considering how well linearly related θ_w and CAPE are (in general), and how poorly linearly related CAPE and flash rates were observed to be. Table 10 shows the R^2 values for θ_w/flash rate regressions.

Table 10. θ_w versus flash rate R^2 values for Kavieng and Kapingamarangi.

θ_w VS. FLASH RATE		
	R^2's	
	KAVIENG	KAPINGA
05 UTC θ_w VS 03-08 UTC FLASH RATE	0.02	0.05
11 UTC θ_w VS 09-14 UTC FLASH RATE	0.009	0.03
17 UTC θ_w VS 15-20 UTC FLASH RATE	0.05	0.03
23 UTC θ_w VS 21-02 UTC FLASH RATE	0.09	0.06
AVG θ_w VS DAILY FLASH RATE	0.02	0.05

While θ_w (like CAPE), seems to be a good indicator of the amount of energy stored within the tropical atmosphere, it cannot account for instances during which lightning activity is either high or low on a persistent basis. The puzzle of weakly electrified oceanic cloud systems has to be examined, then, from a multi-scale point of view. By looking more closely at the effects of water loading, buoyancy changes, height of the LFC, entrainment, and departures from undilute parcel ascent, the conditions leading to liquid condensate reaching the elusive mixed-phase region of a cloud may be better understood.

CHAPTER VI

TIME SERIES ANALYSIS

1. Basic Time Series Techniques

a) Overview and data reconstruction

In this part of the study, the focus is shifted to purely statistical analysis of various lightning time series collected during and after TOGA-COARE. As mentioned earlier, the basis for performing this analysis methodology stems from the fact that the data may exhibit correlation in time. Because of the lack of independence among the quantities investigated, the need arises for a very graphical tool with which to analyze data of this sort (Newton 1988).

The aims of time series analysis are manifold, but can be grouped into four main categories. Basic among these, is a thorough description of the data in question. The remaining objectives deal with spectral density estimations, prediction and statistical inference. Of particular interest in this section of the study is an attempt to describe the pattern that lightning activity exhibits over this part of the tropics from a more statistical point of view.

As alluded to earlier, each data set used suffers from varying degrees of missing data. Therefore, before performing any of the subsequent time series methods, complete sets must be compiled. At Rabaul, for example, data were not collected during seventeen days in October and one day in November. This lack of data is compounded by the fact that each set of daily total flashes is further divided into land

and ocean flashes. As a result, the need arises to reconstruct three data sets for each location instead of just one. Simple linear regression was used in regressing all non-missing days between similar regime series (i.e. total on total, land on land and ocean on ocean). Whenever a "good" linear relationship was observed (i.e., an R^2 above 0.70), its equation was used in filling in the appropriate gaps. If a good linear relationship was not observed, then the land/ocean ratios obtained in **CHAPTER IV** of this investigation were used to fill the gaps. Figure 10 shows six linear regressions using all nine lightning data sets. Clearly, the total flashes and land flashes regressions all yielded good linear relationships while the ocean regressions did not.

Noteworthy is the fact that ***all the days*** used to reconstruct the missing ones (i.e., the *"y's"* and *"x's"* in the equations) fall below 10000 flashes. Because of this, the equations in Figs. 10a-d, seem particularly useful in light of the very good relationship observed towards the low end of the lightning totals (< 10000 flashes). On the other hand, the ocean on ocean regressions (Figs. 10e,f) did not show an acceptable linear relationship. In order to reconstruct these time series, the appropriate land/ocean lightning ratios and predicted land sector values were used. By dividing the predicted land sector values by the land/ocean ratio, estimates of the "ocean" values are obtained. For the Kavieng and Kapingamarangi ocean sector data sets, the appropriate monthly ratios were used. For Rabaul, however, since so many days are missing (seventeen days in October and one in November), an August-September-October average ratio was used. This was deemed as representative of the October ratio due to the similarity in lightning frequency observed during these three months.

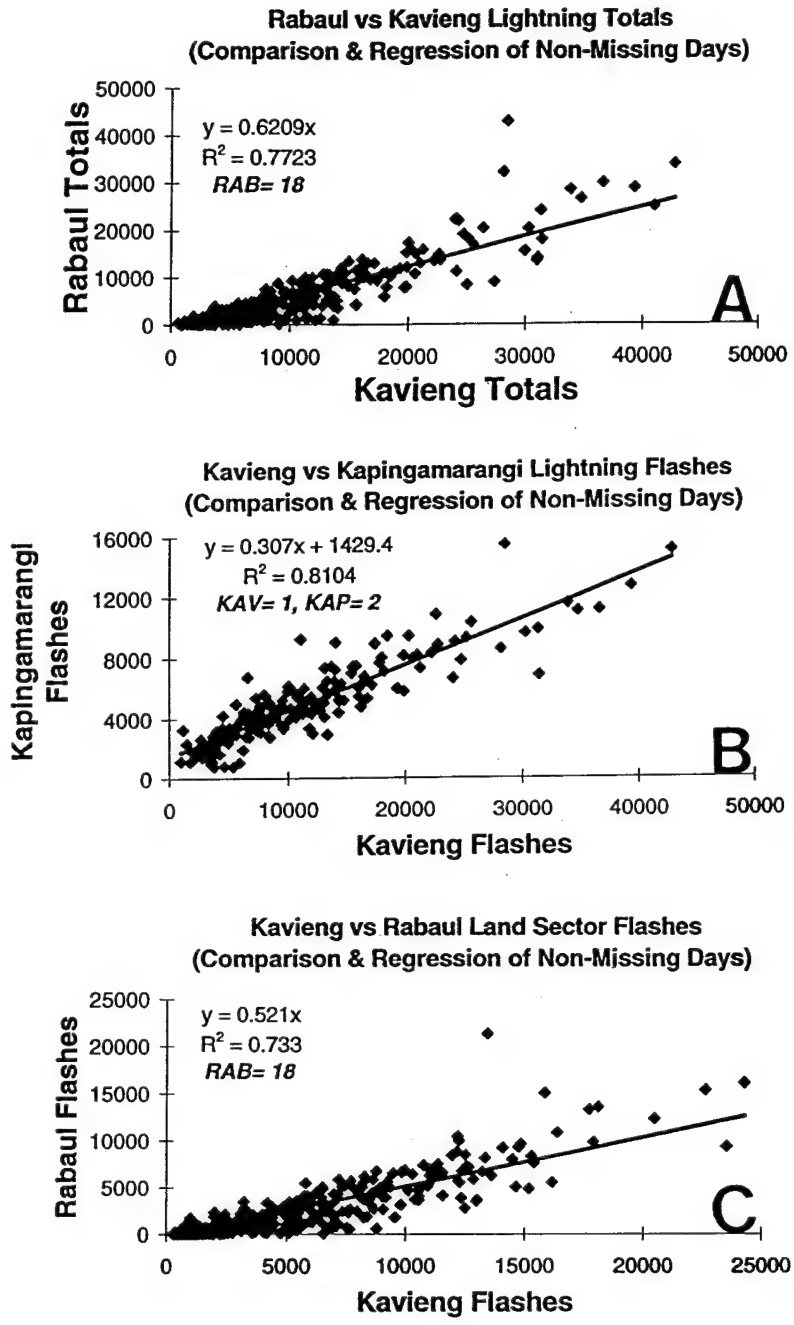

Fig. 10. Six linear regressions using all nine time series; total flashes on total flashes (a&b), land on land flashes (c&d), and ocean on ocean flashes (e&f). RAB = "#", KAV = "#" and KAP = "#" corresponds to how many data gaps each regression was used for.

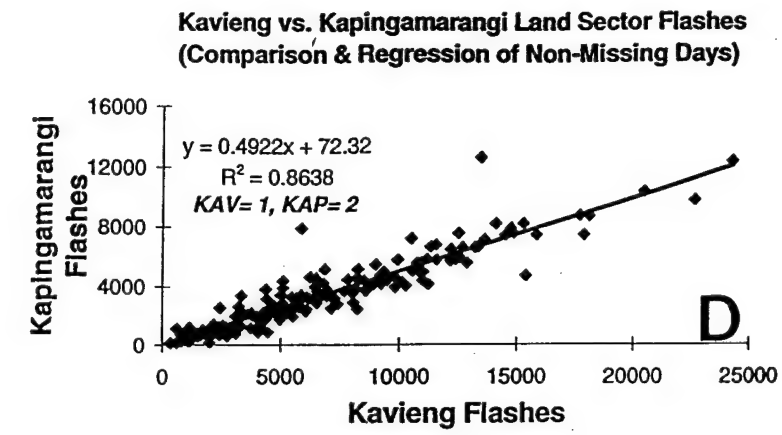

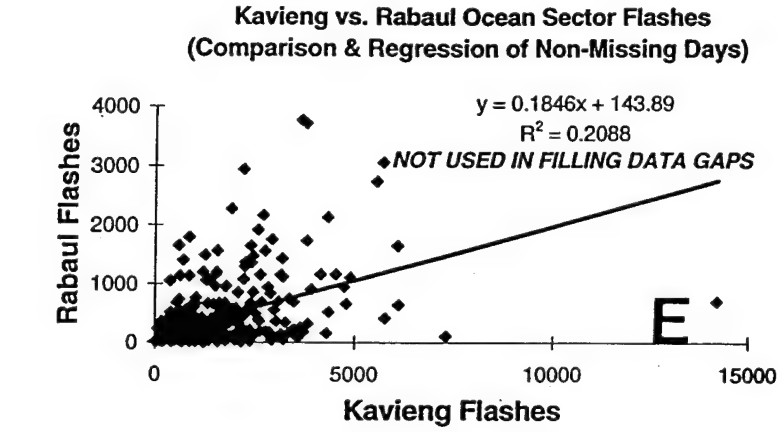

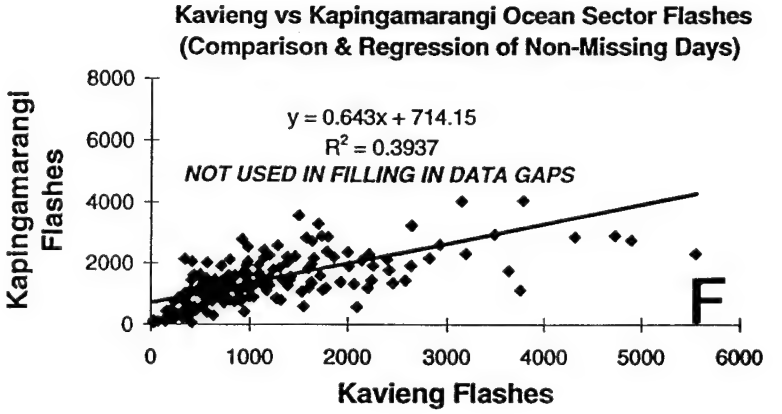

Fig 10. (Continued)

The results of restoring all the time series via the aforementioned methods are shown in Figs. 11a-i.

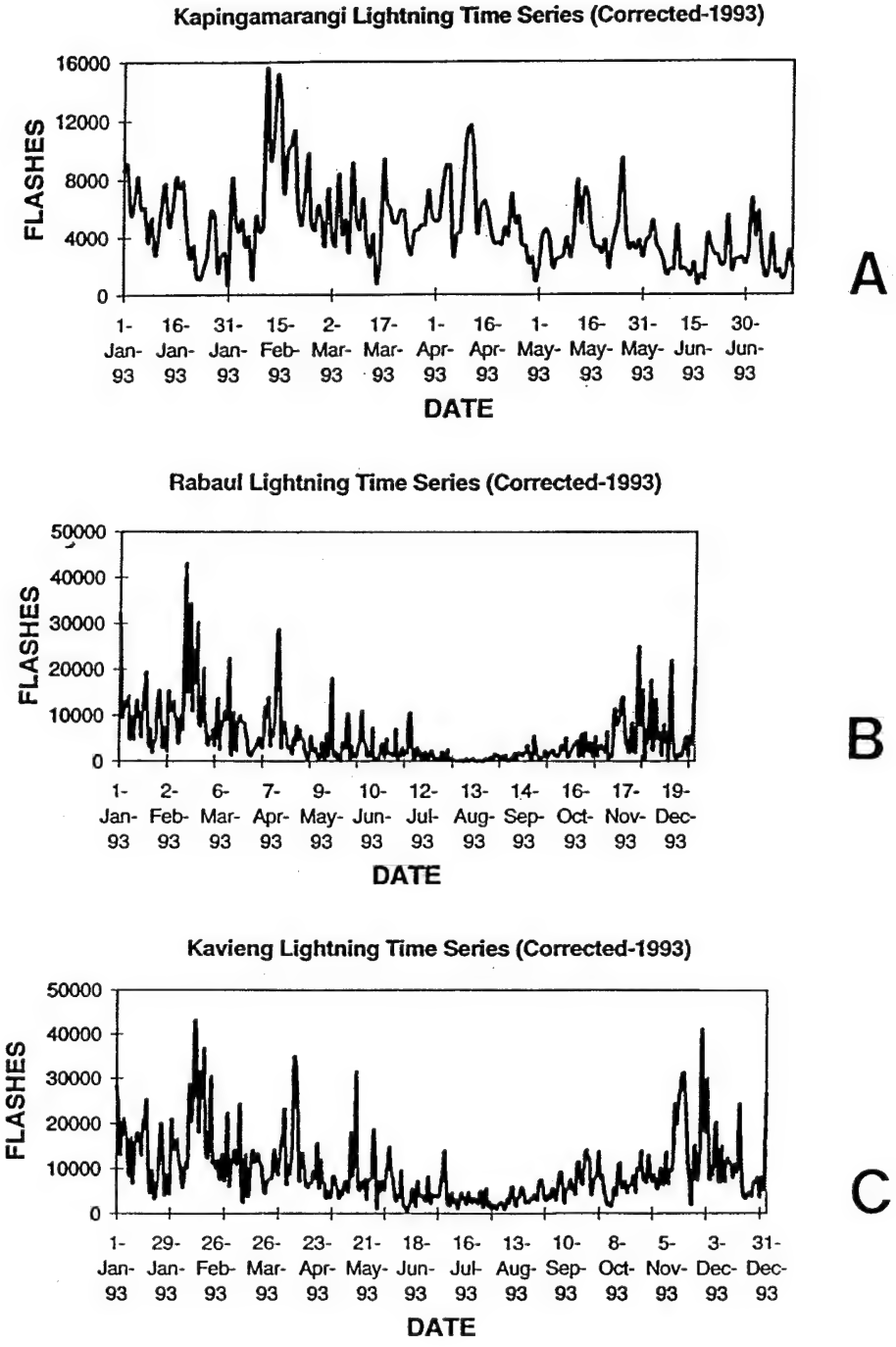

Fig. 11. Restored lightning time series for total flashes (a-c), land sector flashes (d-f), and ocean sector flashes (g-i) for all three DF sites.

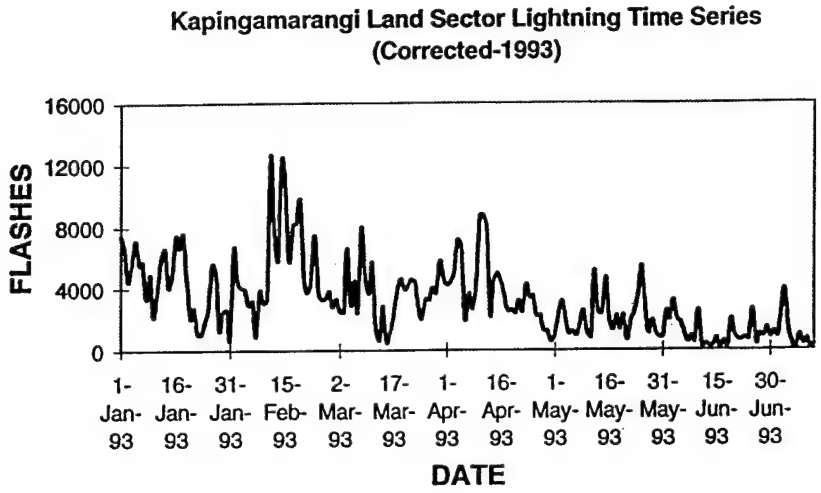

D

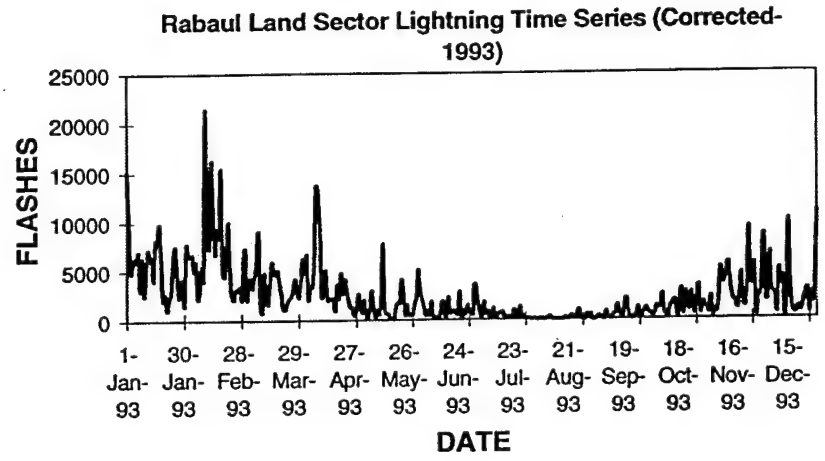

E

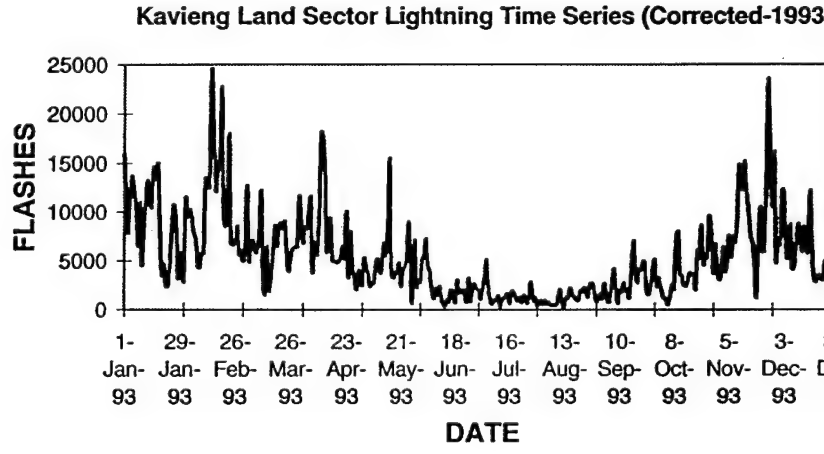

F

Fig 11. (Continued)

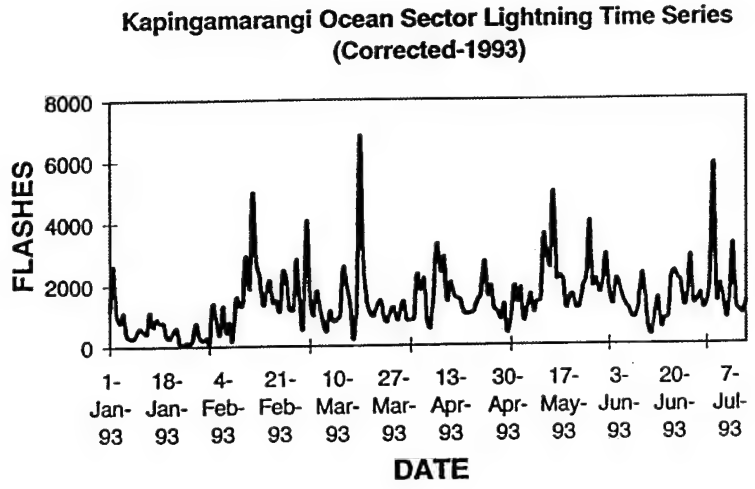

G

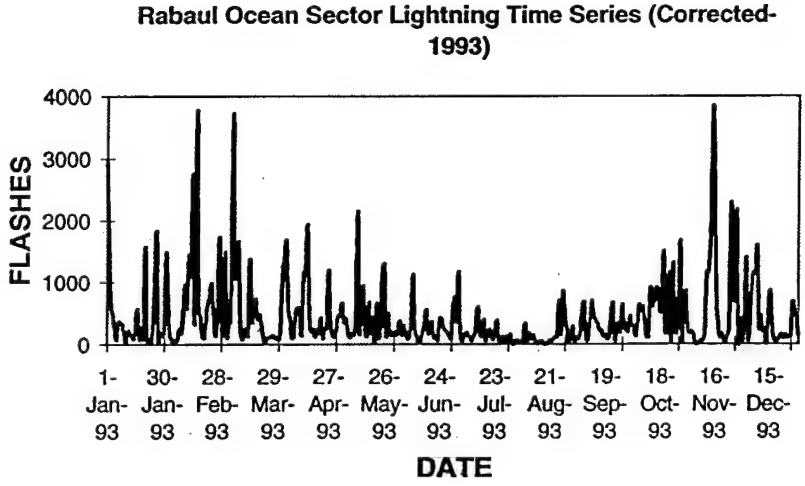

H

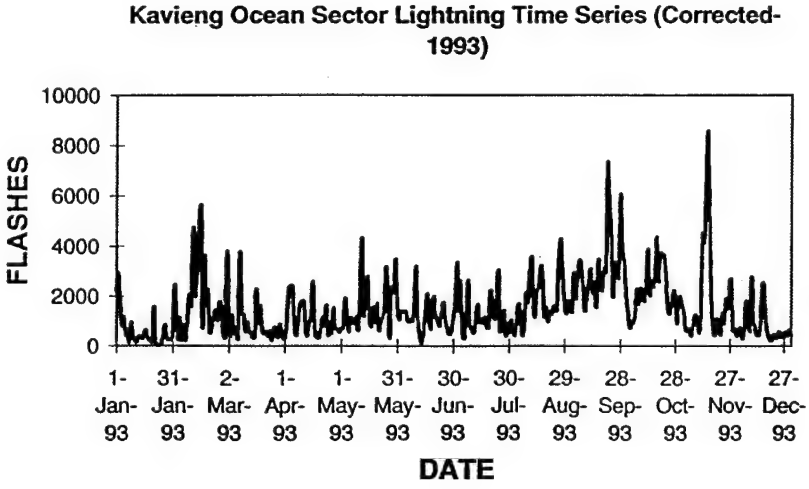

I

Fig. 11. (Continued)

b) Descriptive statistics

One of the most important goals of any statistical procedure is to give a basic, yet thorough, description of the data being analyzed; both numerically and graphically. In time series analysis, there are three basic graphical techniques with which to describe data. These include the sample correlogram, the periodogram and the partial correlogram.

As mentioned earlier, a distinguishing characteristic of a time series is that the data within it can exhibit correlation over time (Newton 1988). If we have a time series *x(1),..., x(n),* one could measure the correlation of the data with themselves (auto-correlation) except lagged a certain number of time units. As a result, for a specific lag v, we can obtain n-v pairs of x's that are separated by v time units. The sample autocorrelation coefficient is then given by;

$$\rho(v) = \frac{\sum_{t=1}^{n-v}(x(t)-\bar{x})(x(t+v)-\bar{x})}{\sum_{t=1}^{n}(x(t)-\bar{x})^2} \qquad (1)$$

where $\bar{x}$ is the sample mean of *x(1),..., x(n).* Note that a plot of $\rho(v)$ versus v for v = *0, 1,...,M* is the sample correlogram, where M is the number of lags used.

Two important purposes of the correlogram are to show whether a periodicity in the data of v time units exists, and to quantify the type of memory series one is dealing with. Time series memory types fall into three categories; white noise, long memory and short memory. A white noise series is one in which no discernible patterns are

seen in the data and where knowing the first observation does not help predict the *(n+1)st* observation. It should be noted that if one encounters a white noise time series, no further analysis methods need be applied since no more information is essentially available. Because of this, all nine lightning time series will be run through a white noise test. A long memory time series, on the other hand, is one which is comprised primarily of deterministic data. In other words, the future is very predictable from the past. Finally, short memory time series fall in between the previously mentioned types and embody the majority of series dealt with in the physical sciences.

Testing the hypothesis for white noise is a very basic, yet crucial step, in the analysis of any data set. The white noise test utilized in this study uses the sample correlogram and the cumulative periodogram in determining whether a series is white noise or not. For such a purpose, 95% confidence bands are superimposed on both graphs. If more than 5% of the correlations $\rho(v)$ *for* $v=0,1,\ldots,M$ or the points in the cumulative periodogram fall outside the bounds, then the white noise hypothesis is rejected. Tests performed on all nine series show that ***all the data within each series are not*** white noise. Figure 12 shows two of the nine tests which represent the extreme cases. Note, for instance, how clearly Rabaul's land sector test (Fig. 12a) falls outside the bounds while Kapingamarangi's ocean sector test (Fig. 12b) does not. This may be characteristic of the fact that while the land and total flashes series display a disturbed periodicity in flash maxima (between 38 and 59 days), the oceans series do not exhibit this feature (see Figs. 11a-i).

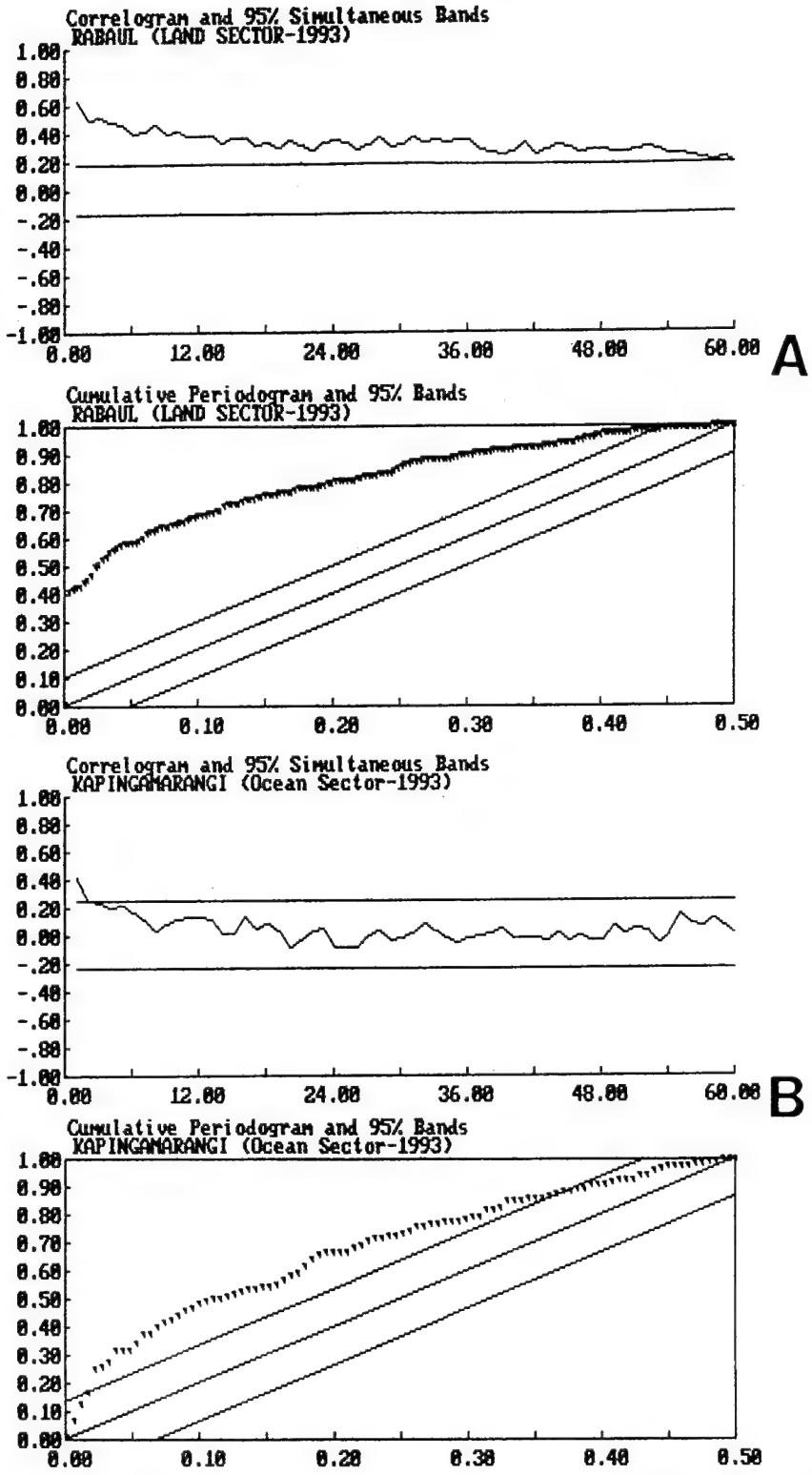

Fig. 12. White noise tests for (a) Rabaul's land sector series, and (b) Kapingamarangi's ocean sector series.

Considering the proximity of the DF's to each other, testing for independence is another natural procedure to submit these data to. Qualitatively, one would expect a pair of equal regime/equal length univariate time series to be highly dependent and highly cross-correlated at lag $v=0$ (i.e., from point to point). The method used to quantify the independence (or lack thereof) of a pair of series is to test the hypothesis that their cross-correlations are zero. A problem arises, however, when **sample** cross correlations appear to be quite high, when, in reality, **true** cross-correlations oscillate about zero. As a result, it is traditional to use the cross-correlations of a filtered version of the original series rather than the series itself in order to test for independence.

Specifically, the chosen test fits autoregressive processes to both univariate series, calculates cross-correlations of the errors and tests whether the cross correlations are significantly different from zero using 95% confidence bands for lags *-M to M*. Tests conducted on all nine series show that all pairings are comprised of ***dependent*** data. Figure 13 shows an example.

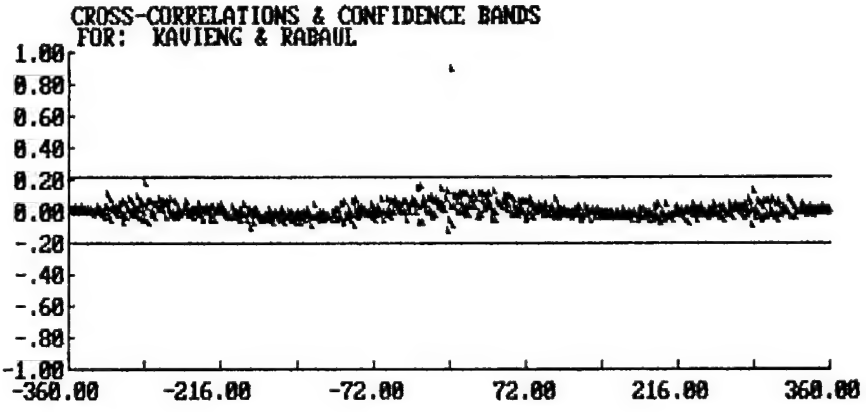

Fig. 13. Example of test for independence.

Note how ***all*** the cross-correlations, ***except for lag zero*** are not far removed from zero and how none of the data points cross the confidence bands. Table 11 shows all the cross-correlations for all nine univariate pairs.

Table 11. Cross-correlations for nine univariate pairings of lightning time series for lag zero.

	TOTAL			LAND			OCEAN		
	Kap/Kav	Rab/Kap	Kav/Rab	Kap/Kav	Rab/Kap	Kav/Rab	Kap/Kav	Rab/Kap	Kav/Rab
Cross-Corr:	0.96	0.91	0.93	0.98	0.95	0.92	0.86	0.64	0.73

After testing for white noise and independence, the attention is again re-focused on the descriptive statistics. The correlograms for all three sites, and flash classifications, (see Figs. 14a-i), all show an eventual decay towards zero with increasing lag. Because of this, one might at first assume each series to be strictly short memory. Closer examination of each correlogram, however, reveals an interesting and important difference between the ocean series and the rest of the series.

Each ocean series (Figs. 14g-i) ***rapidly*** decays to zero (i.e., after about lag v=3 or 4) and oscillates about it thereafter. This fact categorizes these series as your "textbook definition" short memory type. The remaining series (Figs. 14a-f), on the other hand, show a more gradual decay towards zero with significantly non-zero autocorrelation as far out as lag v= 52. This non-zero component to these autocorrelation functions may be due in part to the period range observed through lightning peaks which is noticed to fluctuate between 38 and 59 days. The lack of high autocorrelation between lags 30 and 60 is credited to the fact that the oscillations within these data are not strictly periodic.

Of interest as well is the "sinusoidal" nature of the Kapingamarangi total and land flashes correlograms. This is credited to the fact that only 195 days worth of data are available. Not only is this time interval (1 Jan - 14 Jul 93) the period with the most readily apparent peaks in lightning activity, but little of the data from the convective minimum period (which shows the weakest and least periodic pattern of the year; July through September) is sampled. Because of this, the result is that Kapingamarangi's total, and land flashes correlograms sinusoidally decay towards zero unlike its Kavieng, and Rabaul counterparts. This difference notwithstanding, each series in Figs. 14a-f is classified as a hybrid between short memory and long memory, showing characteristics of both.

The next significant descriptive statistic to study is the periodogram. A periodogram describes the sinusoidal decomposition of a time series by rewriting the series as a sum of sinusoids of periods, n, $n/2$, $n/3$,..., $n/[n/2]$ or frequencies $1/n$, $2/n$,...,$[n/2]/n$. Conventionally, it is generally accepted that periodograms are plotted as a function of the log of the amplitude versus frequency. Herein lies the idea behind basic harmonic analysis in which a unique set of sinusoids, when added together, mathematically represent the data set being studied. This technique allows an investigator to study complicated data sets by breaking them into simpler "frequency components" and studying them separately. Also, this method allows for the extraction of information otherwise masked to the eye by noise (Newton 1988). In order to obtain these sinusoids, the data within each series are fourier transformed.

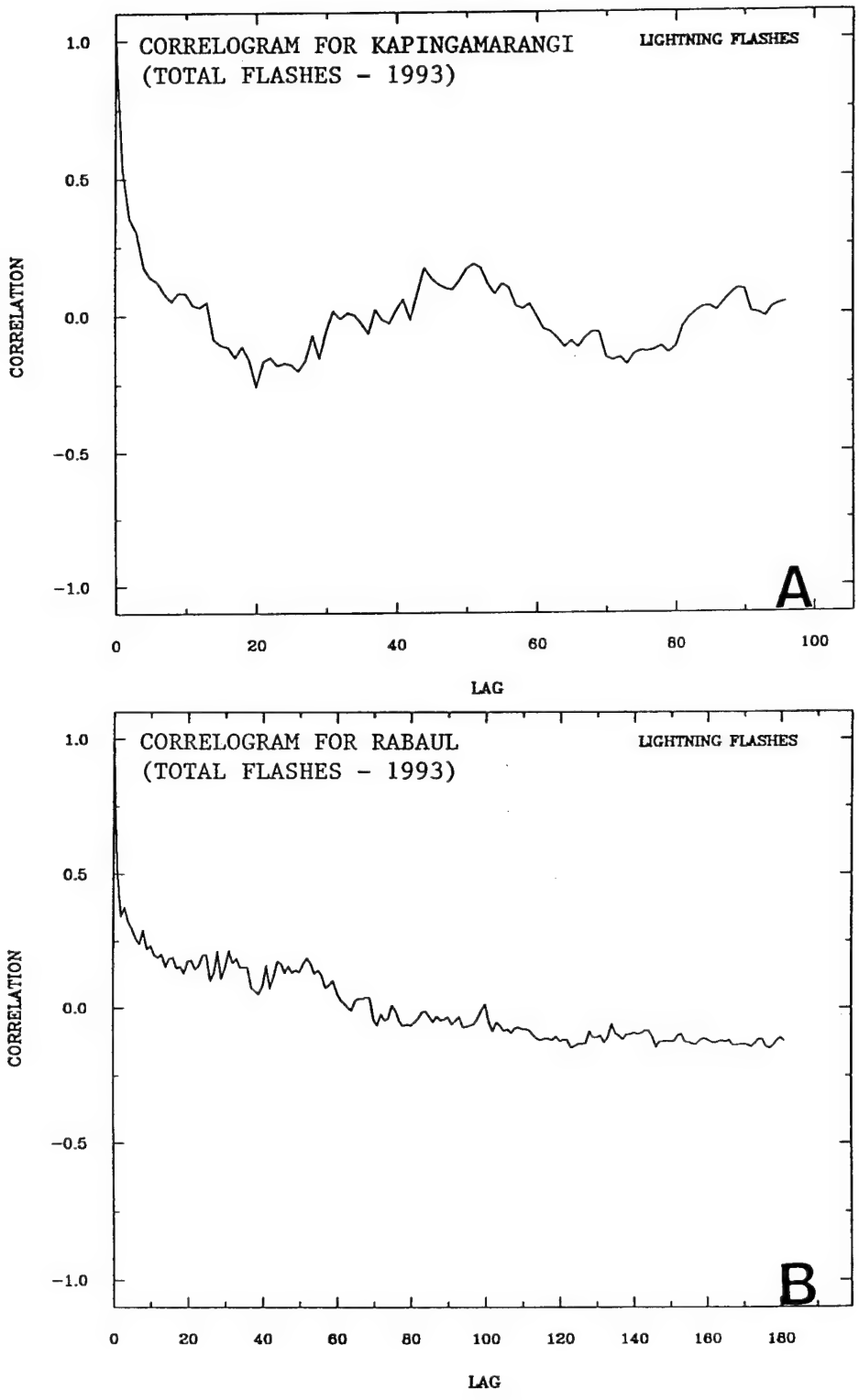

Fig. 14. Correlograms for all nine series (a-i). The abscissa represents the lag (in days) for $v=1,...,M$, and the ordinate the correlation coefficient (for each series, M was chosen as the number of data points divided by two).

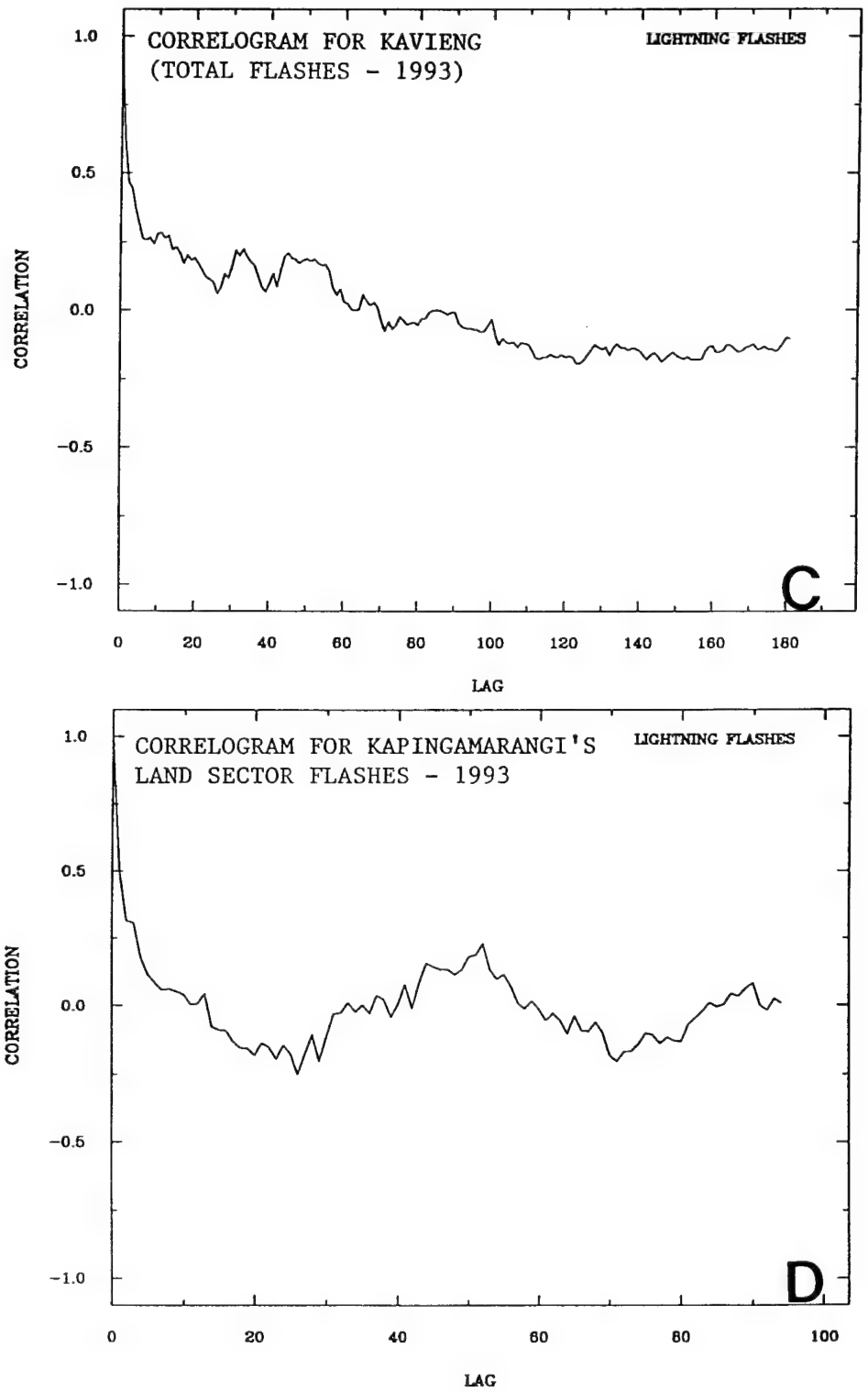

Fig. 14. (Continued)

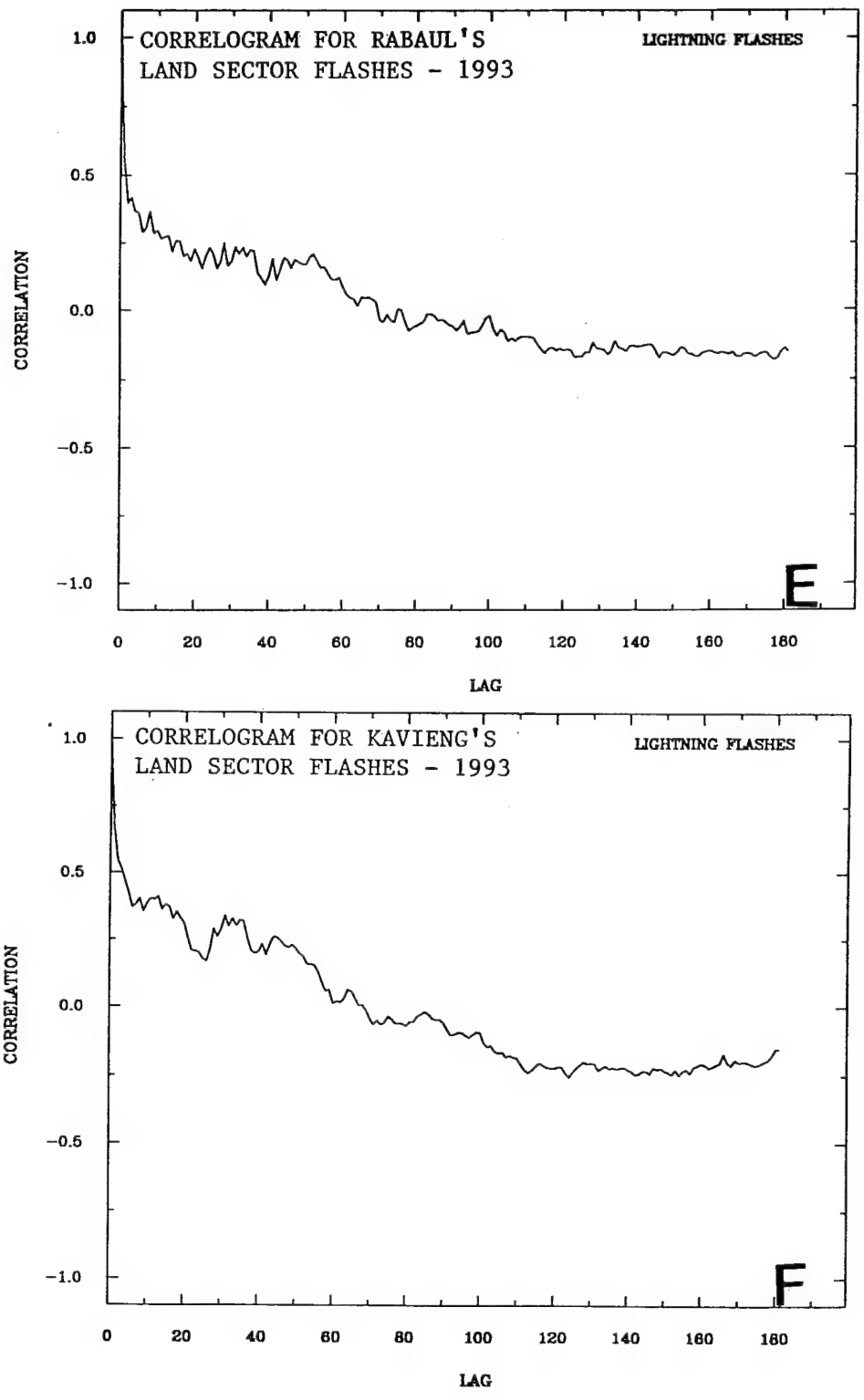

Fig. 14. (Continued)

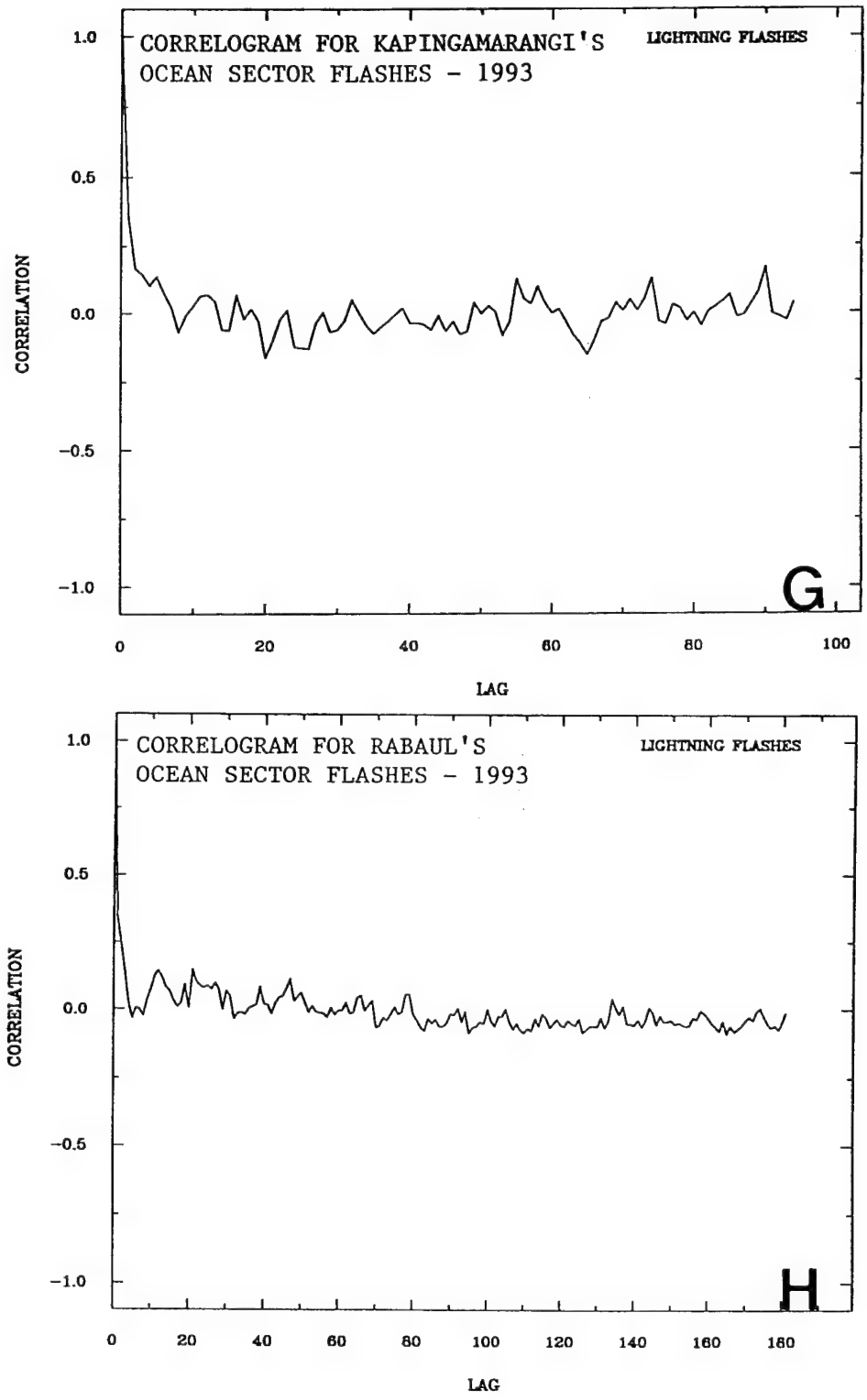

Fig. 14. (Continued)

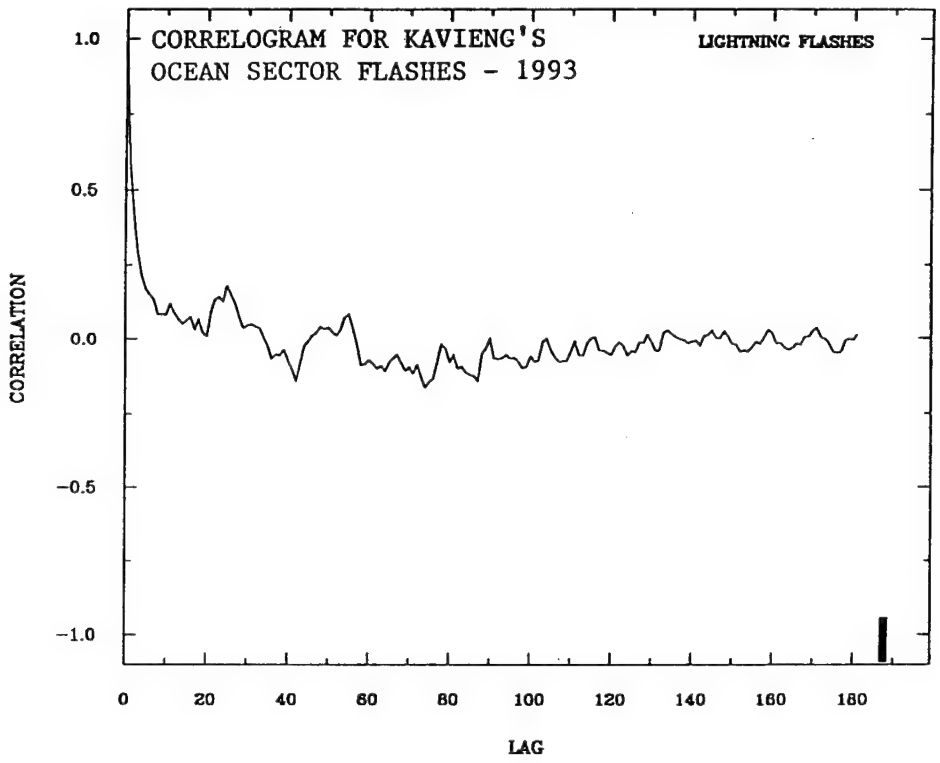

Fig. 14. (Continued)

That is to say, if we let *x(1),...,x(n)* be n numbers, the discrete fourier transform ofthose numbers is the set of complex numbers *z(1),...,z(n)* given by;

$$z(k) = \sum_{t=1}^{n} x(t) \cos 2\pi (t-1)\omega_k + i \sum_{t=1}^{n} x(t) \sin 2\pi (t-1)\omega_k \qquad (2)$$

where; $\omega_k = \frac{(k-1)}{n}$, for $k=1,...,n$ over the interval *[0,1/2]*

Figures 15a-i shows how the total flashes and land series are particularly characterized by an excess, however slight, of low frequency (i.e., long periods tend to dominate). As mentioned earlier, periodograms help pick out the amplitudes of the component sinusoids. Since, in general, time series data are not strictly composed of sums of sinusoids, one can only make qualitative statements regarding the data. For example, note how, in general, no ***one*** fundamental frequency is observed within any of the series while the low frequency domination is only apparent after careful examination. Only after looking closely at the periodograms does one notice how the amplitudes (or power) of the high frequencies (< 0.10 day^{-1}) are large relative to any other frequency.

As was the case with the correlograms, differences are noted between the periodograms of each series regime. The periodograms for the ocean flashes series show that they are less strongly dominated by high frequencies with a rapid oscillation about a constant beyond approximately frequency 0.05 day^{-1}. This is less apparent in the total, and land flashes series. Although cyclic data sets will, by definition, have peaks in their periodograms, the fact that lightning data within any regime do not show

show any ***strict*** periodicity, essentially eliminates the possibility of peaks, as is indeed the case.

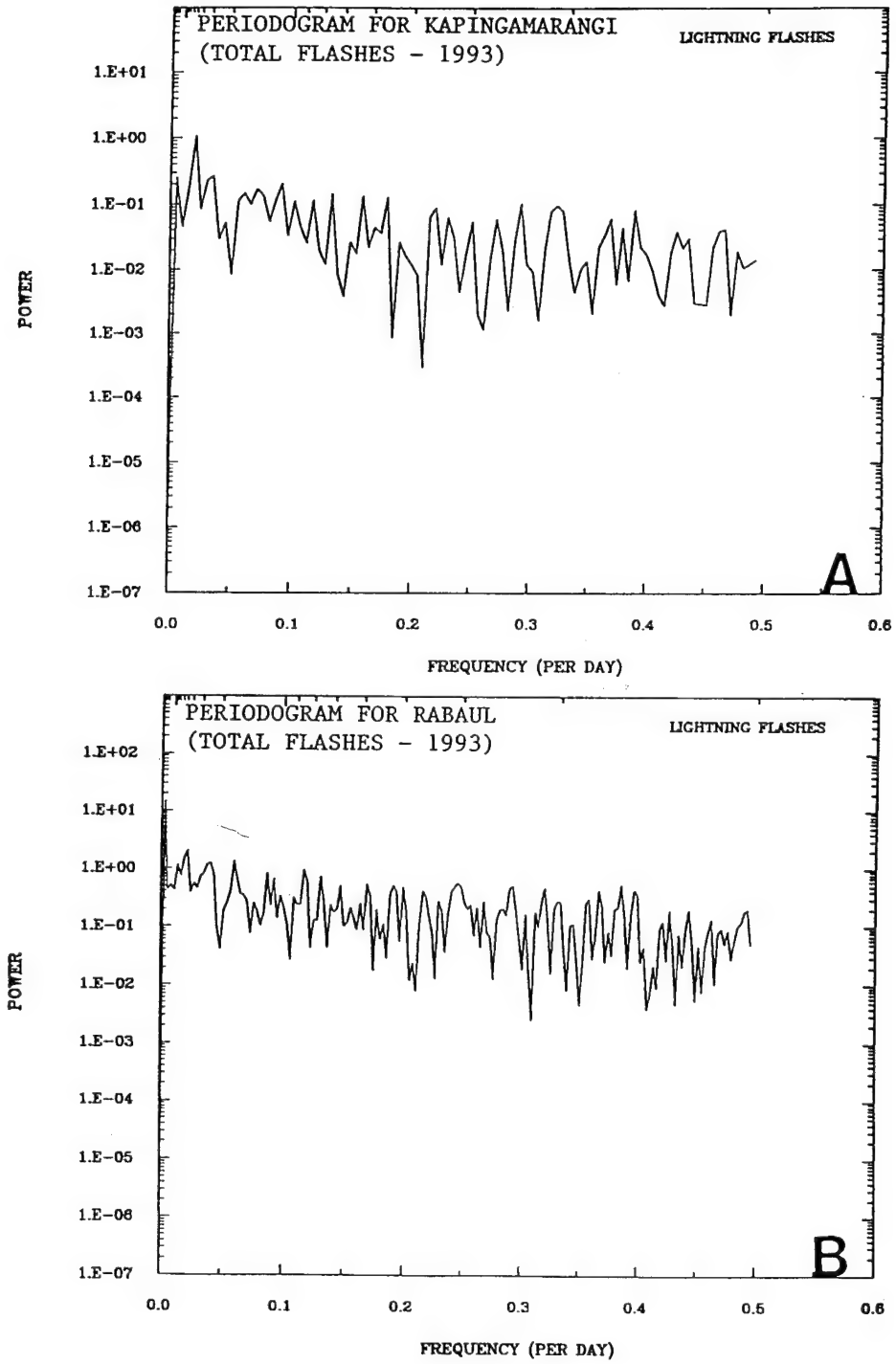

Fig. 15. Periodograms of all nine series (a-i). The abscissa represents the frequency range [0,1/2], and the ordinate is the log of the amplitude.

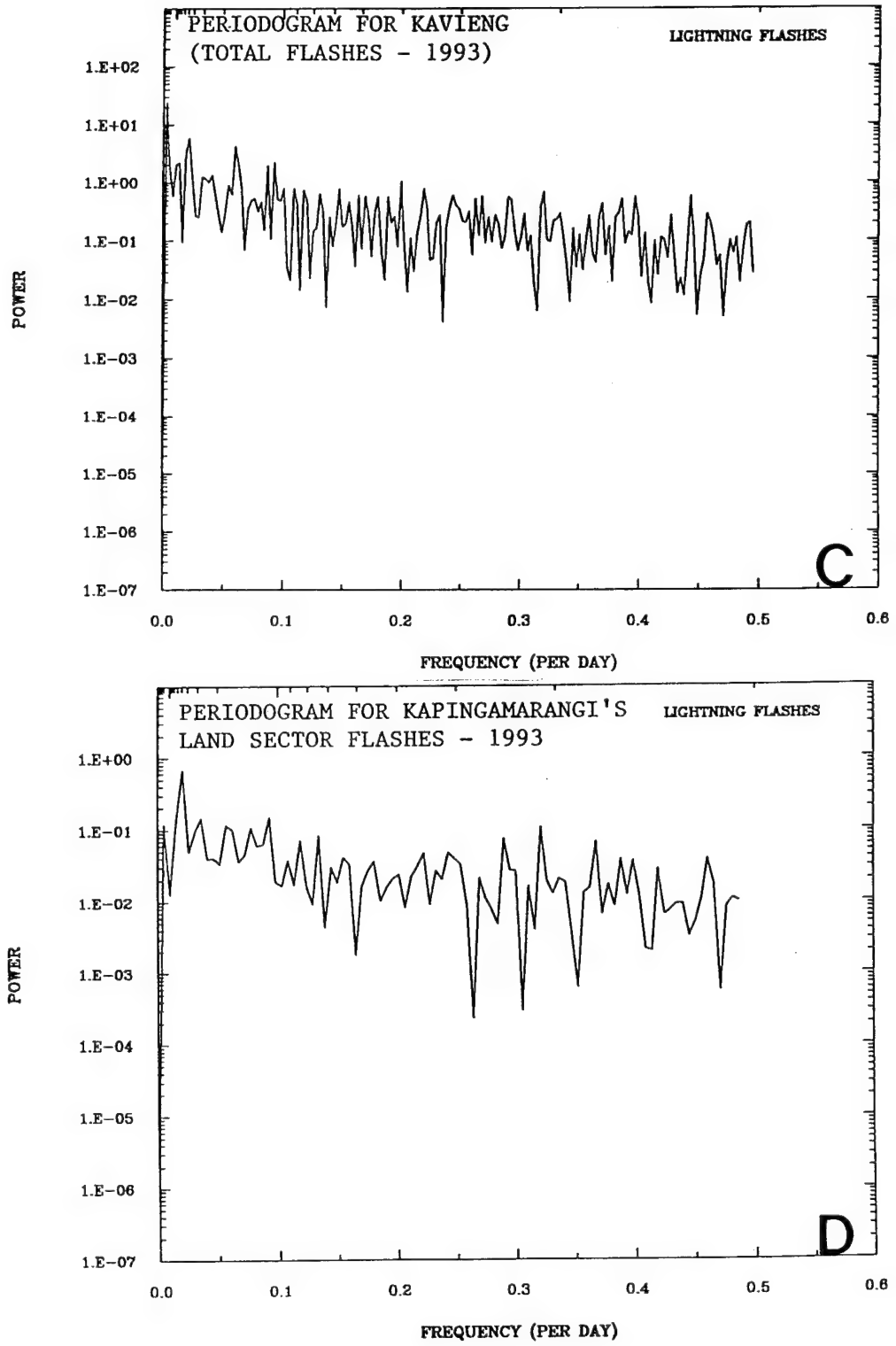

Fig. 15. (Continued)

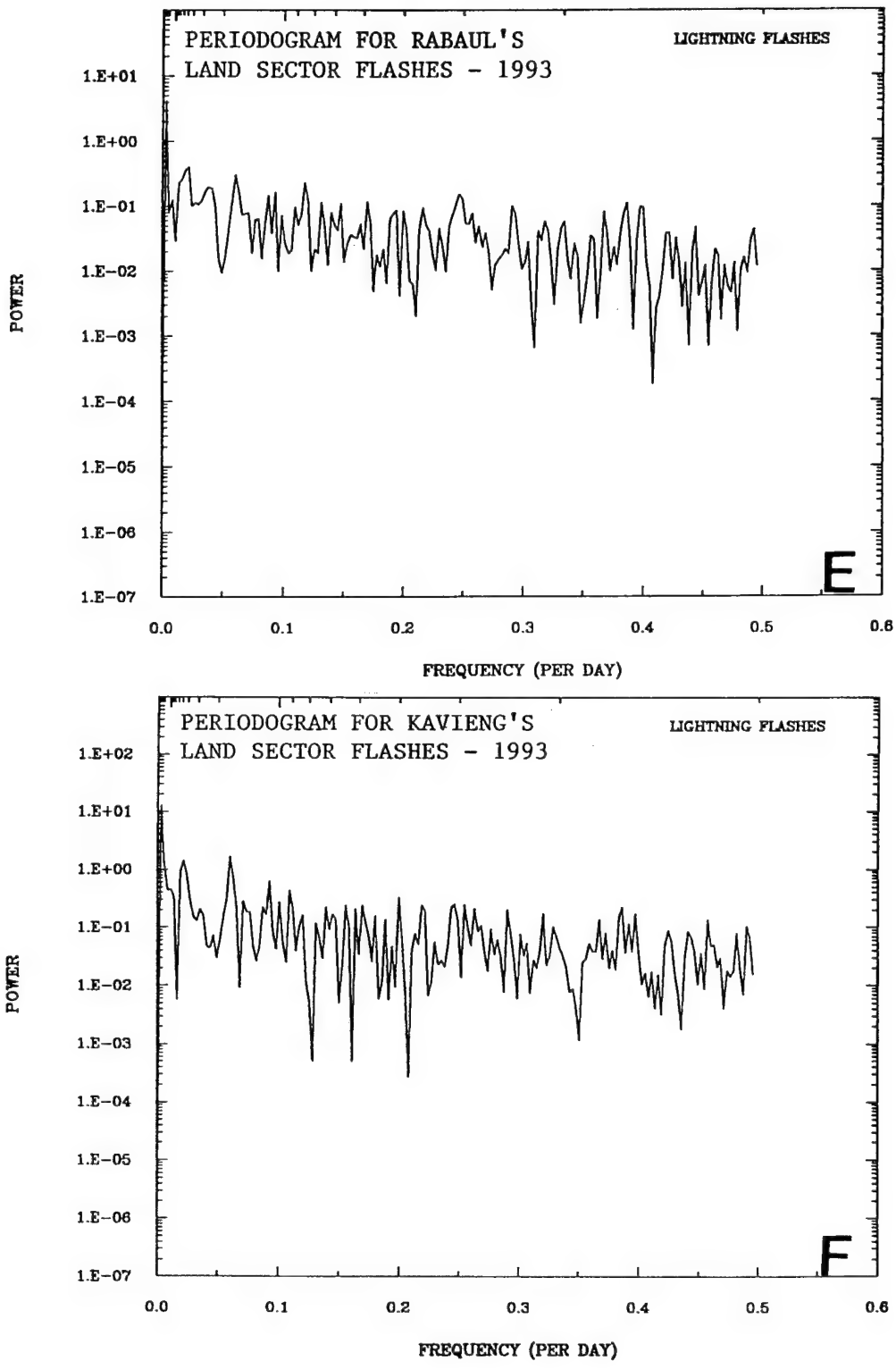

Fig. 15. (Continued)

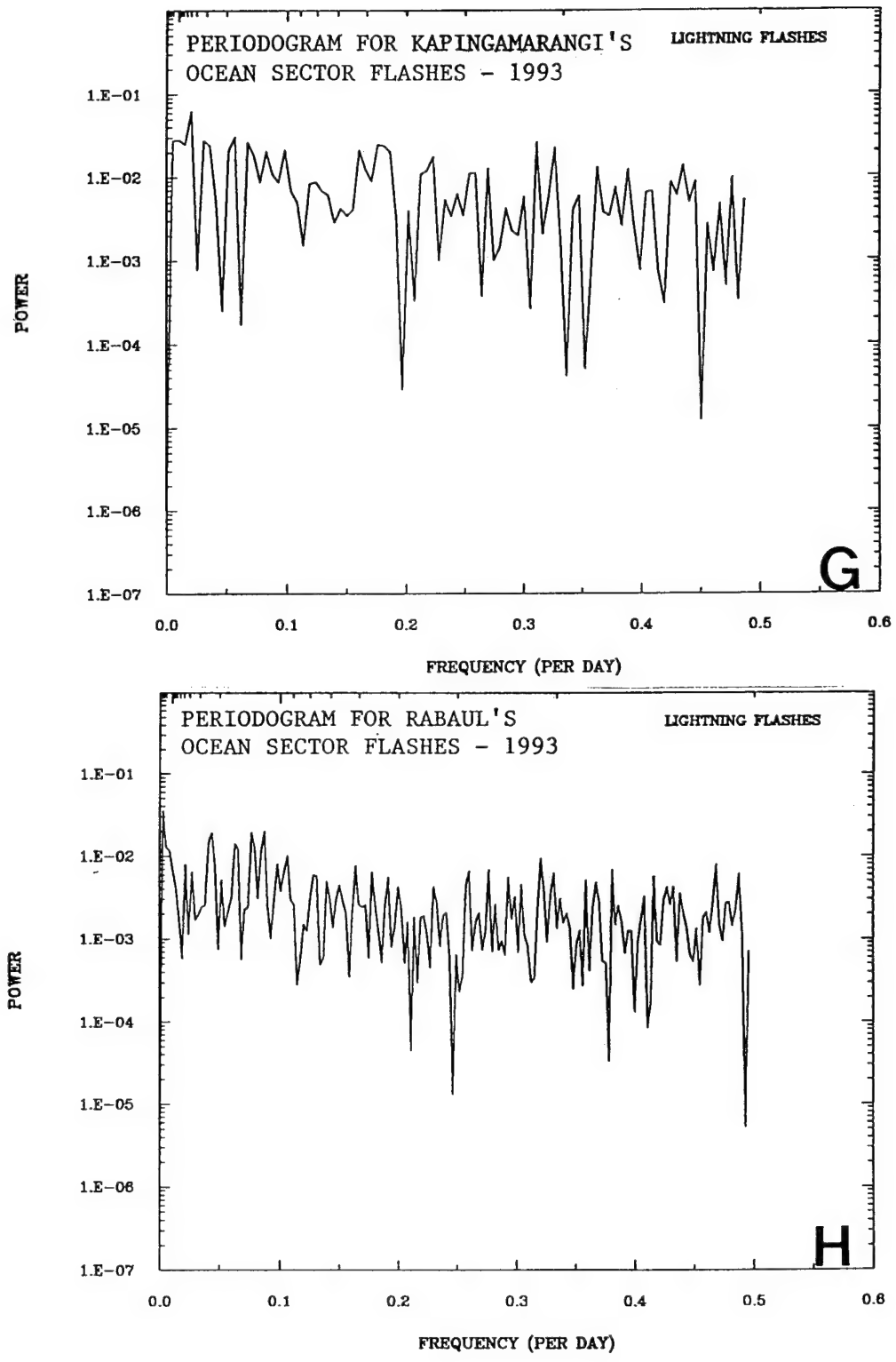

Fig. 15. (Continued)

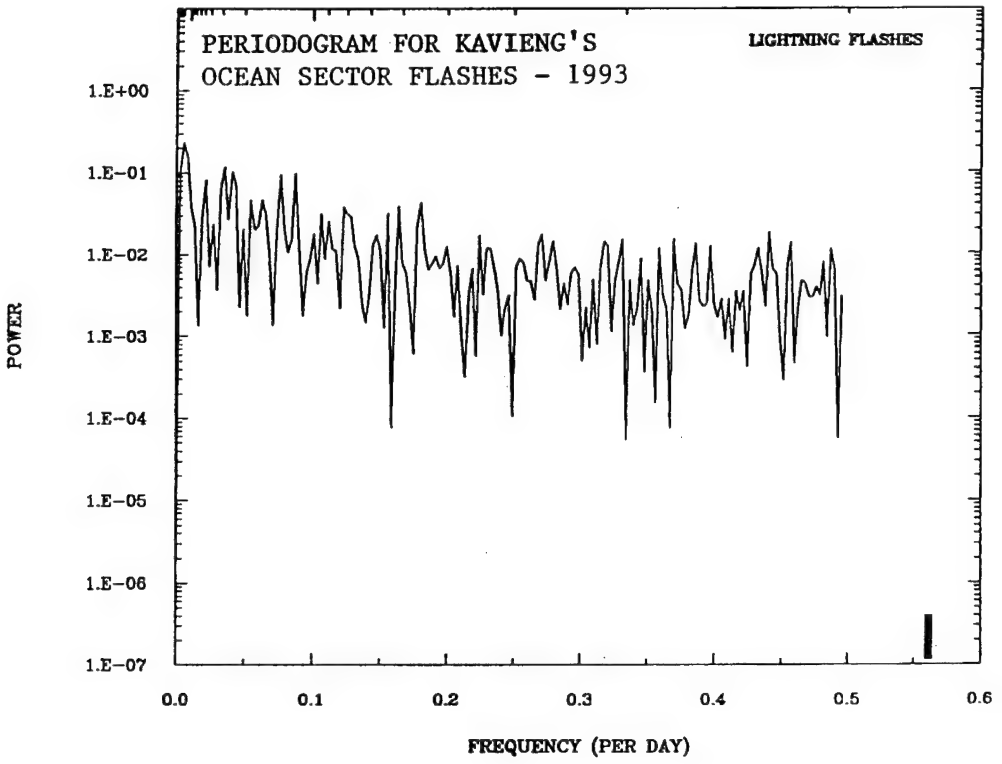

Fig. 15. (Continued)

The last of the descriptive statistics to be discussed in this study is the partial correlogram. This statistic, denoted by $\hat{\theta}(v)$, is the sample correlation coefficient of *x's v* time units apart, but after having removed the effect of the *x's* in between. In other words, any possible influence that the variables in between may have on the coefficient. Along with partial autocorrelations, one can examine the residual variances. These are simply the sample variances of the residuals having regressed *x(t)* on the previous *"v" x's* (Newton 1988). By dividing the residual variances by the sample variance, one obtains standardized residual variances. The latter are plotted along with the partial autocorrelations and serves to indicate what memory type a particular series is.

Figures 16a-c shows partial autocorrelations and standardized residual variances for three series chosen as representative of their specific regime. Note the similarities between Figs. 16a,b, for example. In both of these there is relatively high partial autocorrelations for lags *v= 1* and *2* with a sharp drop off and an oscillation about a constant thereafter. Standardized residual variances show a range in value between 0.62 and 0.50 for both a and b highlighting, once again, the in-between short and long memory characteristics of flashes within these regimes . In Fig. 16c (ocean sector series), however, note how much lower the partial autocorrelations are for lags *v=1 and 2* while the standardized residual variances increased in value from approximately 0.83 to 0.70. As mentioned earlier, the ocean series exhibit traits that more closely ***resemble*** white noise. In reality, the ocean series are classic short memory types, and

therefore tend to show weaker partial autocorrelation and higher standardized residual variances, as the data indeed show.

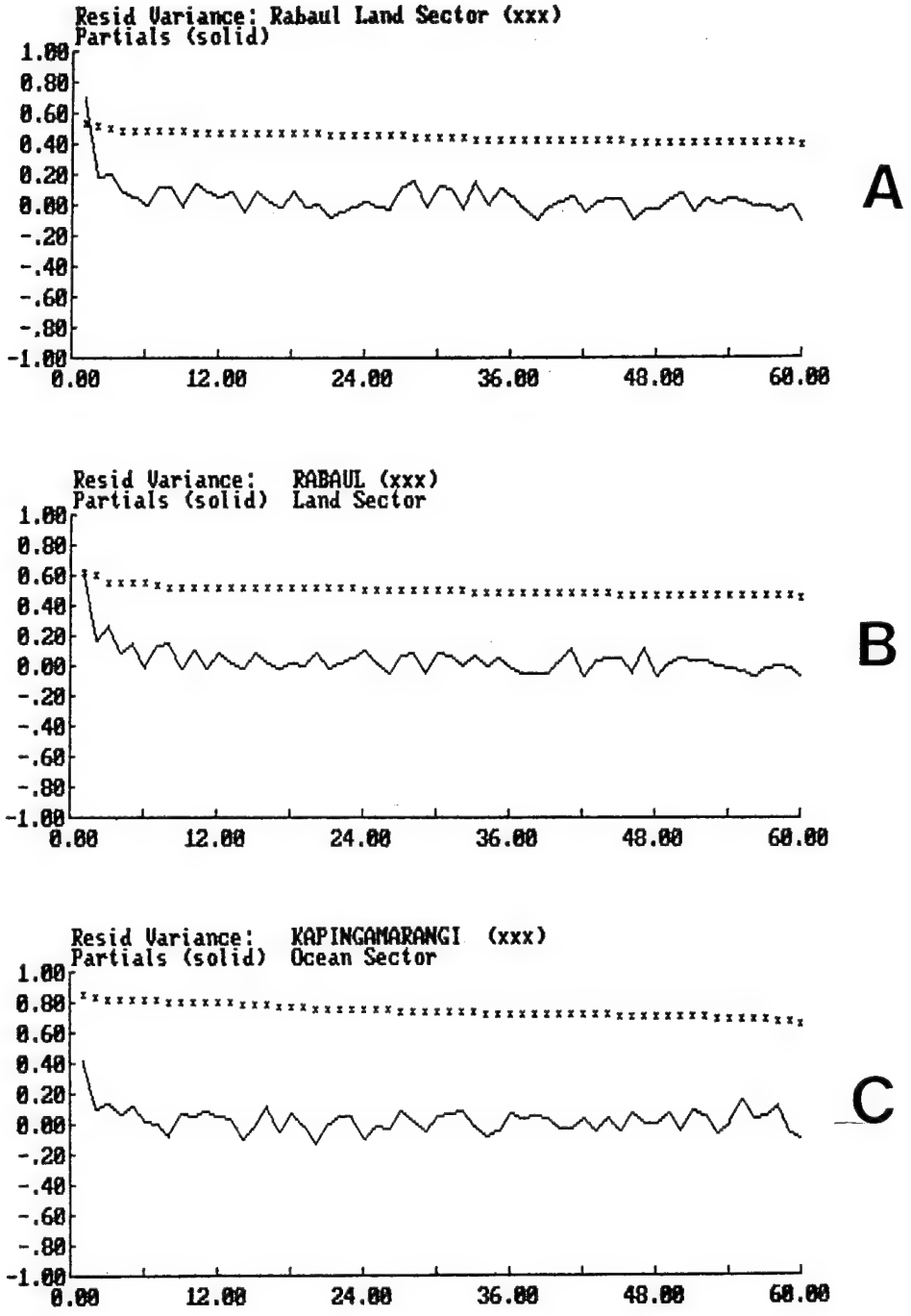

Fig. 16. Partial autocorrelations and standardized residual variances for three series chosen as representative of their particular regime. The abscissa represents the lags $\nu=1,\ldots,M$ and the ordinate the partial autocorrelation coefficient.

2. Lightning and the Madden Julian Oscillation

a) Filter construction and selection

A qualitative examination of daily flash counts for ***total*** and ***land*** flashes series reveal distinct peaks in lightning activity that occur between 37 and 59 days (first observed by Lucas and Orville (1994)) during the period 1 January 1993 through the beginning of July. Thereafter, lightning activity displays a more erratic pattern with no readily apparent period range. The main objective of this part of the investigation is to study the lightning data under the ***assumption*** of a 30 to 60 day period interval. This is attempted in an effort to see whether the MJO signature is detectable through the use of OLR anomalies and filtered lightning data. Part of the motivation behind the use of OLR anomaly data, besides their readily available nature, centers around the well documented notion that they are strongest over the eastern Indian and western Pacific Oceans (Knutson et al. 1986; Knutson and Weickmann 1987).

In order to filter out the data not belonging to the aforementioned period range, a band-pass filter was constructed with maximum response at 40 days (0.025 day^{-1}), bounded between 30 and 60 days (i.e., the 0.03333 to 0.01667 day^{-1} frequency interval). It is stressed that no trends or cycles were removed from any of the data. Instead, the ***original*** data sets were run through the filter which removed any unwanted higher frequency oscillations (such as a 10-15 or 20-25 day cycle) present within them. The objective is to obtain "smoothed" series that pick out the desired information (lightning peaks) for use in the comparison with OLR anomalies. Note in Fig. 17, an example of such a filter. The vertical lines (which form a box) represent

the ideal bandwidth chosen while the smoother curve, known as the transfer function, is used to approximate the ideal band-pass filter. Simply stated, the transfer function is a weighting function to the chosen frequency spectrum allowing only a certain amount of energy to enter the filter as a function of frequency. In other words, each frequency is weighted accordingly with the center frequency given the strongest weight.

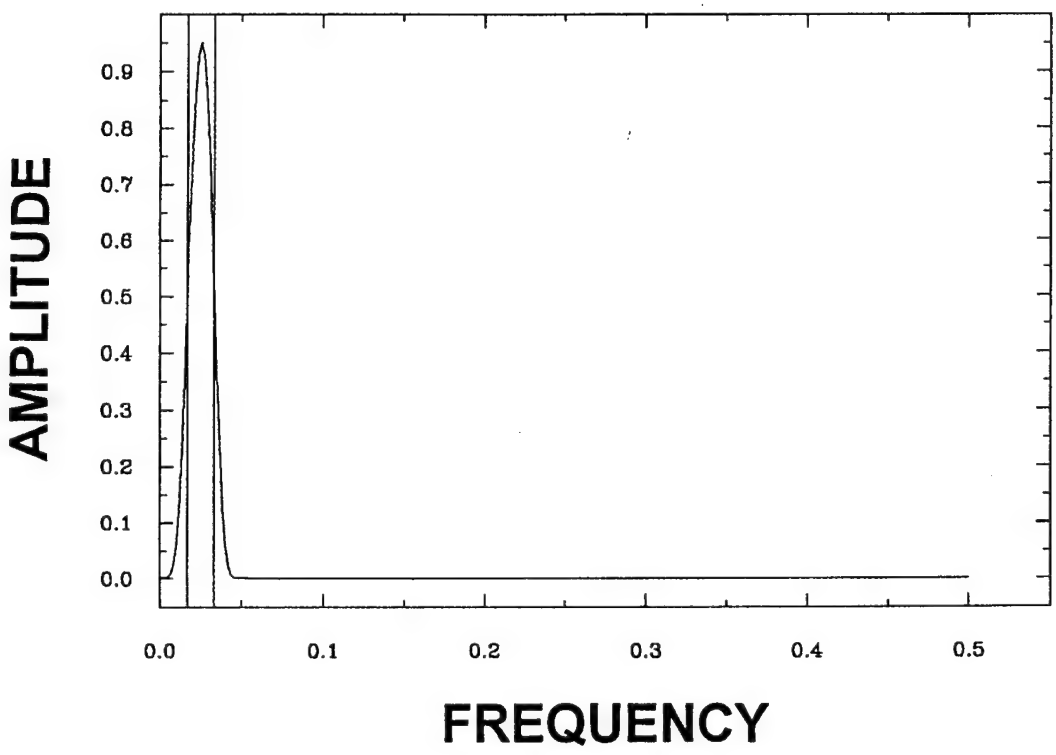

Fig. 17. Band-pass filter.

Although the basic premise for using the aforementioned filter remains, it is noteworthy to explain why this particular filter was chosen above any other. The lightning data were run through several other filters of varying parameters to establish which one worked best (i.e., which one best patterns the lightning data). Table 12 shows a summary of each filter and its parameters. Tests using the four filters

Table 12. Filter parameter comparison.

FILTER	RANGE [Frequency Range] (Period Range)	MAXIMUM RESPONSE (In frequency) (In days)	BANDWIDTH
1	**[0.03333 to 0.01667 day^{-1}]** **(30 to 60 days)**	**[0.025000 day^{-1}]** **(40 days)**	**0.008333 day^{-1}**
2	[0.02700 to 0.01690 day^{-1}] (37 to 59 days)	[0.022222 day^{-1}] (45 days)	0.005038 day^{-1}
3	[0.02500 to 0.01667 day^{-1}] (40 to 60 days)	[0.020800 day^{-1}] (48 days)	0.004167 day^{-1}
4	[0.02850 to 0.01538 day^{-1}] (35 to 65 days)	[0.021978 day^{-1}] (46 days)	0.006557 day^{-1}

reveal very similar patterns, although filter number one showed the best results. Because of this, and because its 30 to 60 day range matches the characteristic time scale proposed by Knutson and Weickmann (1987), it was selected.

b) Filter results (all regimes)

The result of filtering the Kavieng time series is shown in Fig. 18a with the filtered data superimposed on total flashes along with a graph of total, land and ocean filters (Fig. 18b). Notice the weakening of each filtered series past late June and their subsequent re-intensification towards early November and how the filters essentially hover around zero from late July through most of September (during the observed convective minimum). The pattern observed during the year, especially the first half, is reminiscent of an oscillation in the data with MJO's classic 30-60 day time scale signature. Even after re-intensification, the pattern is not as well defined as it was earlier in the year. Particularly interesting is the fact that all three filters are clearly in "phase" during January through July, and how thereafter, they are clearly not. This same pattern is very similar to the one observed at Rabaul (not shown here).

Although this limited-data study does not prove (nor attempts to prove) any ***seasonal*** dependence of lightning activity on MJO, the data available (both filtered and unfiltered) suggest that any possible MJO-lightning link might be strongest during the Northern Hemisphere winter and spring months. Table 13 shows how much of the total variance is explained by the chosen bandwidth. Note how the variance in lightning activity accounted for by the filter variance varies from 2.7% to 15.3% throughout the three-DF domain. The larger percentages result from the total and land filters and

Table 13. Percentage of total variance explained by filtered series variance.

	Kapinga			Kavieng			Rabaul		
	Total	**Land**	**Ocean**	Total	Land	Ocean	Total	Land	Ocean
$\sigma_{fs}^2/\sigma_{ts}^2$:	**15.3%**	**13.6%**	**7.3%**	8.9%	9.5%	4.7%	7.1%	8.6%	2.7%

from the Kapingamarangi data. These results point to a higher degree of coherence between the lightning flash data and the filter data during roughly the first half of the year; the period which exhibits the most prominent and consistent peaks in lightning activity. Since the Kapingamarangi data are only available for the first 195 days of 1993, its time series accentuates this observation.

Figure 18 was compared with OLR anomalies (obtained from the Climatic Diagnostics Bulletin, December 1993 issue) in an attempt to confirm whether its cycles are indeed reasonable. The assumption here is that the part of the MJO oscillation experiencing more convective activity (negative OLR anomalies) is, in turn, subject to increased lightning activity.

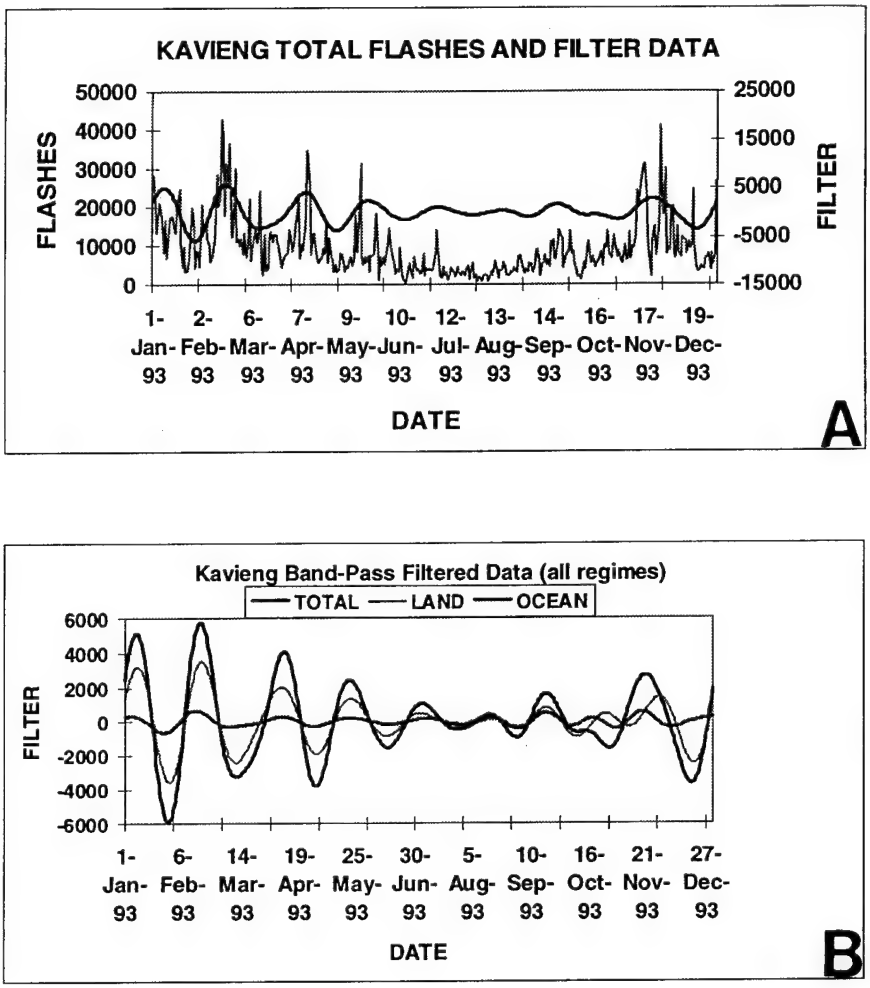

Fig. 18. Filtered Kavieng series superimposed on total flashes (a). Total, land, and ocean filters (b) for Kavieng.

In the next diagram (Fig. 19), the solid black line represents the average longitude of the three DF's used in the comparison of filtered lightning data with OLR anomalies. Recall that ***total*** and ***land*** flashes series were found to be very well cross-correlated for lag 0 (see Table 11), with their peaks matching to within plus or minus two days for the first five months of the year (Table 14). As a result of this similarity, a mean date corresponding to filter peaks is used in the comparison with OLR anomalies. Thereafter, however, the differences in times of peaks exceed five or more days, and each series is examined separately. In Fig. 19, the *"**X**'s"* mark the locations corresponding to the observed peaks in lightning activity as computed by the filter for ***Kavieng's total flashes series***. Out of all the peaks observed during the year, only the first four (January through July) seem to ***approximate*** areas of negative OLR anomaly maxima. Beyond this point, however, the relationship (inexact as it is) weakens. This is true of both total and land series for Rabaul and Kavieng. Table 14 shows a compilation of all filter peaks for individual DF site and flash classification.

Qualitative examination of the ocean flashes series for all three locales does not suggest the same distinctive pattern of peaks with an obvious period range (to the naked eye, that is). Were it not for the fact that the ocean series fail the white noise test (see Fig. 12b), one might even dismiss these series as not possibly having any connection to MJO. Running the series through the filter, however, reveal a very similar pattern to that obtained by the total and land filters, with a signal that is much weaker in amplitude throughout the year (see Fig. 18b). Although it is quite obvious

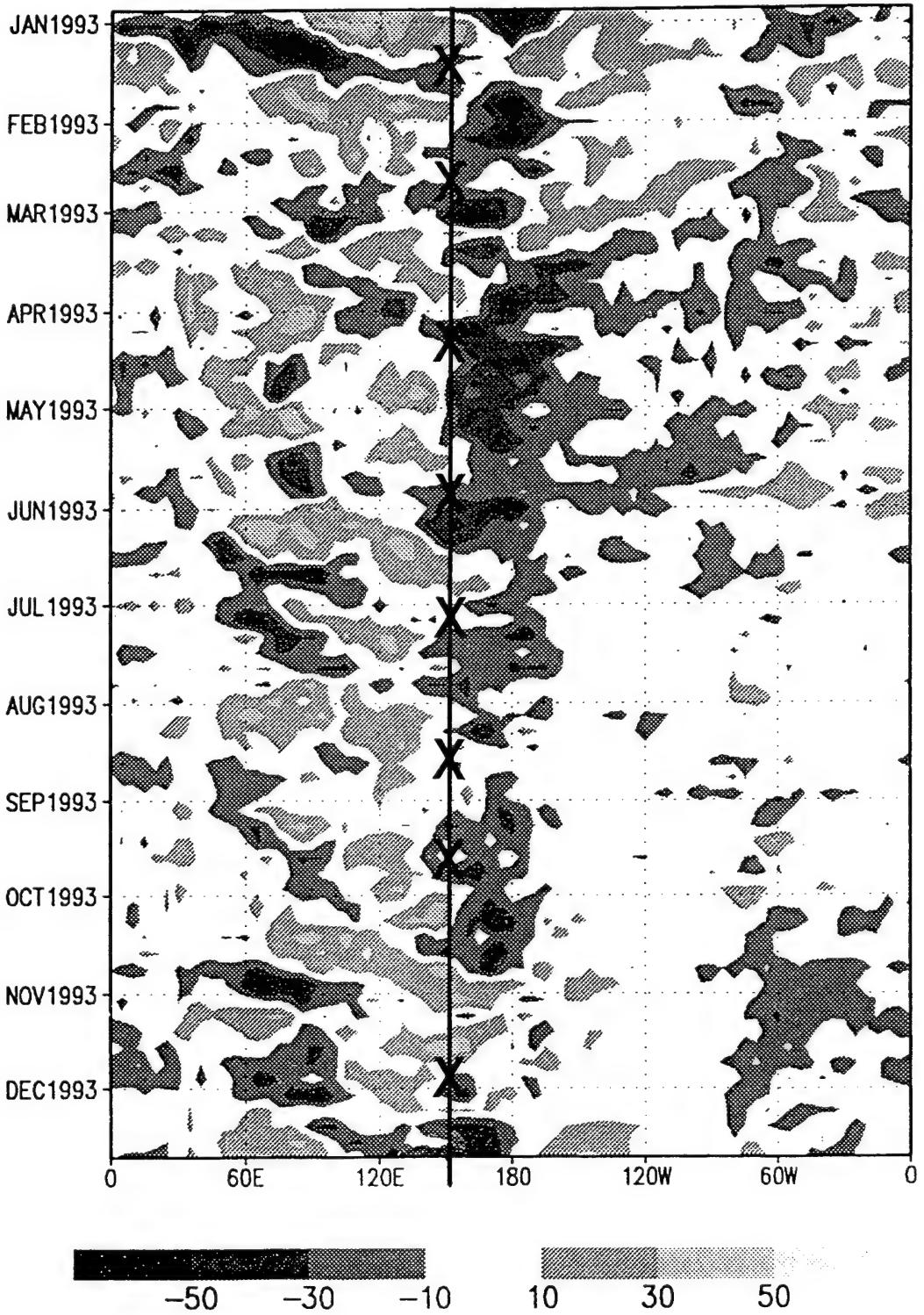

Fig. 19. Time-longitude section (5°N-5°S) of anomalous OLR (Adapted from the Climatic Diagnostics Bulletin, December 1993 Issue). Anomalies are computed for each pentad (average of 5 day period) with units of W m^{-2}. The solid black line represents the average longitude of the three DF's while the "X's" correspond to the peaks in the filtered Kavieng total flashes series.

Table 14. Filter peak dates for all three locations.

KAPINGAMARANGI									
Total	9 Jan	16 Feb	9 Apr	24 May					
Land	10 Jan	17 Feb	9 Apr	24 May					
Ocean	No Peak	15 Feb	11 Apr	20 May					
KAVIENG									
Total	8 Jan	16 Feb	9 Apr	24 May	4 Jul	15 Aug	20 Sep	No Peak	20 Nov
Land	9 Jan	17 Feb	9 Apr	25 May	3 Jul	18 Aug	20 Sep	26 Oct	28 Nov
Ocean	5 Jan	14 Feb	9 Apr	20 May	8 Jul	16 Aug	19 Sep	18 Oct	18 Nov
RABAUL									
Total	9 Jan	15 Feb	11 Apr	24 May	4 Jul	9 Aug	13 Sep	14 Oct	27 Nov
Land	9 Jan	15 Feb	11 Apr	25 May	5 Jul	19 Aug	16 Sep	16 Oct	29 Nov
Ocean	4 Jan	No Peak	12 Apr	18 May	3 Jul	No Peak	6 Sep	17 Oct	22 Nov

that the ocean series are classic short memory series (i.e., their correlograms rapidly decay to zero and stay there), comparing its filter peaks to OLR anomalies is only slightly less informative than the previous attempt.

Figure 20 shows the same time-longitude section of anomalous OLR for 1993 with the "***X***`s", this time, representing the filter peaks computed for Kavieng's ocean flashes series as an example. Again, as in the Kavieng total flashes example, the relationship is best seen during the first half of the year, although as previously stated, the amplitude of the signal is much weaker.

Although the original assumption was that negative OLR anomalies, and, therefore, more convection, would translate to observed peaks in lightning activity, this link is seen to be very subtle (at best) and confined to the Northern Hemisphere winter through spring time interval. Various factors are involved in this determination. First, the lightning data are spatially limited while the OLR data are both spatially, and temporally averaged over a large domain. This difference,

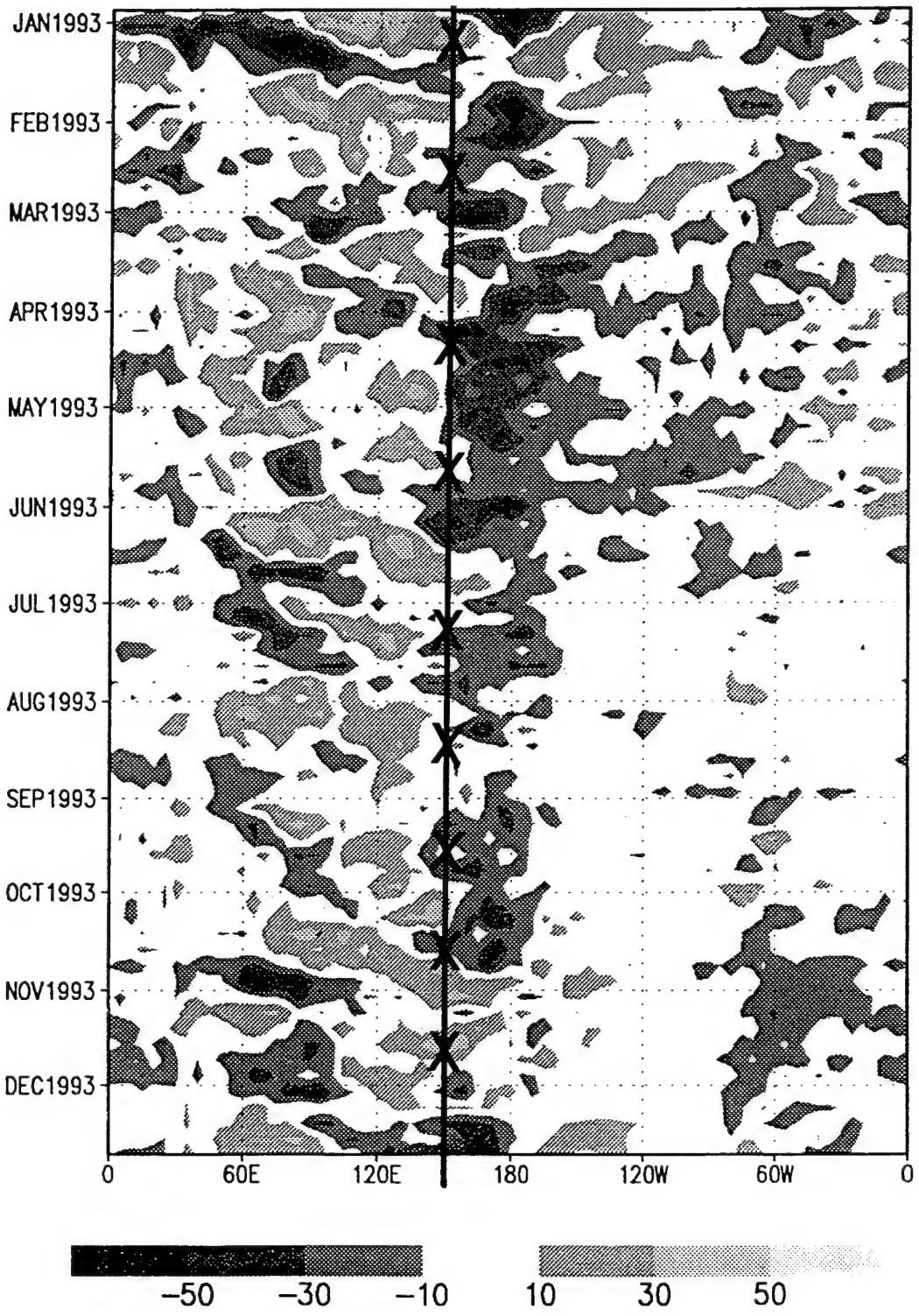

Fig. 20. Same as Figure 19, but for Kavieng's ocean flashes series.

inasmuch as anything, leads to uncertainty, as one is not able to categorically link lightning activity to MJO. Also, Knutson and Weickmann (1987) show that convection anomalies associated with the 30-60 day oscillation are typically centered north of the equator during the Northern Hemisphere summer months. This suggests that as the monsoon moves north, responding to the seasonal cycle of maximum solar radiation (Chang and Krishnamurti 1987), the OLR anomalies move north as well. This results in a weakening of the OLR anomaly signature shown in the Hovmoller diagram which is itself only averaged from 5°N to 5°S. Diagram limitations and the stationarity of the lightning data prevent one from "following" the monsoon north. Therefore, one can only assume the lightning-MJO link (as seen through OLR anomalies) to be similarly defined throughout the year, with significant variations from latitude to latitude within the equatorial tropics. Finally, the observation that oceanic storms are weakly electrified may contribute as well. Although research has shown that convection over this part of the tropics can organize itself into large complexes, these may or may not be electrically active. Therefore, significant convection, from an OLR standpoint, may not necessarily correspond to the most vigorous lightning activity within a given area.

CHAPTER VII

CONCLUSIONS AND RECOMMENDATIONS

As stated in the introduction, the primary objective of this research was to provide a picture of the pattern exhibited by lightning activity over the equatorial region of the warm pool western Pacific Ocean (TOGA-COARE region) for 1993. This main objective was pursued from three different points of view, each offering some insight into the characteristics of lightning activity over a spatial domain scarcely scrutinized before.

The lightning data collected at the Kapingamarangi Atoll, Rabaul, and Kavieng were divided into total, land, and ocean daily flash counts and examined for basic lightning parameters. Also, the same flash count divisions were used in a time series analysis as well as in assessing the possible link between lightning activity and MJO. The thermodynamic portion of this investigation involved studying the spatial and temporal distributions of several parameters in addition to investigating lightning location data for a chosen lat/long box against these parameters.

1. Conclusions

The conclusions drawn from the results follow:

1) Land to ocean ratios of lightning range from an average high of nearly eleven in January to a low of less than one (more ocean flashes) during June through September (time period of observed convective minimum). This is observed to be concurrent with an increase in the percentage of time (per month) that ocean flashes

exceed land flashes. The overall pattern matches that of Orville and Henderson (1986) in implication, though not in average monthly values. The differences in the results are attributed to the differences in the studies.

2) A higher percentage of positive flashes was recorded by the Kapingamarangi DF. At all three locations, however, percentage of positive lightning figures are higher than those typically recorded in the CONUS. These higher values are credited to a combination of nature (advection and in situ mechanisms in the trailing stratiform region of a cloud system), and to equipment sensitivity resulting from the increase in each DF's range.

3) The data show that multiplicity values over the TOGA-COARE region exhibit a pattern similar to that observed in the CONUS. Positive multiplicities range from 1 to 1.2 while negative multiplicities show more variability (1.4 to 2.0). The lowest multiplicities for either category occurred during the convective minimum months of July through October.

4) Histograms of lightning data versus time (LST) show that activity is remarkably more prevalent during the late evening and early morning hours as indicated by a broad maximum peak. This broad peak is apparent in every temporal and spatial category studied. The land sector data at Rabaul show secondary peaks around 1400 LST, while Kavieng's data show broad and pronounced increases in activity commencing early in the afternoon and leading up to the broad nighttime maximum. These features are not apparent in Kapigamarangi's land sector data or in any of the ocean sector data. This points to the diurnal cycle of heating playing a role in the convective cycle of this area as governed by thunderstorm activity forming over

the larger islands. The results agree with convection studies using cloud cluster data (Williams and Houze 1987; Mapes and Houze 1993), and are remarkably different from results gathered at several locations in the CONUS..

5) The distribution of θ_w and CAPE (both temporal and spatial) was observed to be most reliable at Kavieng as evident through average values. This points to data quality as a significant limiting factor in this part of the investigation.

6) The computed CAPE and θ_w values versus varying flash rates proved inconclusive from the standpoint of "high-CAPE (or θ_w)-to-high-flash rate." Both attempts revealed a complete lack of correlation.

7) Time series analysis of total, land, and ocean daily flash counts reveal that none of the data are white noise. Instead, the ocean data were found to be classic short memory series, while the total and land data were observed to exhibit some long memory traits resulting from a modulation in flashes that ranges from 37 to 59 days.

8) The Madden Julian Oscillation was detected through the use of filtered lightning data and OLR anomalies. The link, however, is deemed subtle possibly stemming from differences in the data sets and weakly electrified oceanic storms. The MJO signature is seen in all filtered series, and it is strongest during the Northern Hemisphere winter and spring months. The signal amplitude of the ocean filters is significantly weaker than either of the other two.

2. Recommendations

Based upon the results of the various methods and procedures used throughout this investigation, the following recommendations are suggested:

1) Test different land/ocean sectors to see what, if any, changes from those used in this study become apparent. In addition, a comparison of 1-DF analyses against the same parameters computed for a multi-DF study might prove useful in better assessing the reliability of 1-DF data sets in instances when only single DF's are available (e.g., the single DF that is available at Lajes Field, The Azores, Portugal (with which I worked) and which sits alone in the east central Atlantic Ocean).

2) Upon collection of the new thermodynamic data set, computations of CAPE and CINE using all three available procedures (pseudoadiabatic, reversible with and without ice) is recommended in order to better assess the recommendation by Williams and Renno (1993) who pose the question, *"How should CAPE be calculated for tropical soundings?"* The temporally and spatially rich data set that is forthcoming from NCAR should prove instrumental in this endeavor.

3) Fit statistical models to the lightning time series and attempt prediction with them. Conduct a multivariate time series analysis of the available data.

4) Extend the MJO-lightning link study to examine the DUNDEE lightning data in order to compare those results with TOGA-COARE's. Readily available daily OLR data available from NCAR would facilitate the extension of OLR anomaly data beyond the 5°N-5°S Hovmoller diagram limit and down to Darwin's 12°S latitude.

5) Incorporate the available 1992 and 1993 TOGA-COARE lightning into any of the above recommendations.

REFERENCES

Alexander, G. D., and G. S. Young, 1992: The relationship between EMEX precipitation feature properties and their environmental characteristics. *Mon. Wea. Rev.,* **120,** 554-564.

Brook, M., R. W. Henderson and R. B. Pyle, 1989: Positive lightning strokes to ground. *J. Geophys. Res.,* **94**, 13 295-13 303.

Chang, C. P., and T. N. Krishnamurti, 1987: *Monsoon Meteorology*, Oxford University Press, New York, pp. 203-231.

Dong, Y., and J. Hallett, 1992: Charge separation by ice and water drops during growth and evaporation. *J. Geophys. Res.,* **97,** 20 361-20 371.

Emanuel, K. A., 1994: *Atmospheric Convection,* Oxford University Press, New York, pp. 169-174.

Engholm, C. D., E. R. Williams and R. M. Dole, 1990: Meteorological and electrical conditions associated with positive cloud-to-ground lightning. *Mon. Wea. Rev.,* **118**, 470-487.

Gamache, J. F., 1990: Microphysical observations in summer MONEX convective and stratiform clouds. *Mon. Wea. Rev.,* **118,** 1238-1249.

Griffith, J. M., and E. J. Zipser, 1993: A comparison of the properties and surface fluxes associated with the inflow and downdraft air of tropical MCSs. *Proc., 20th Conf. on Hurricanes and Tropical Meteorology,* San Antonio, TX, Amer. Meteor. Soc., 209-212.

Illingworth, A. J., 1985: Charge separation in thunderstorms: Small scale processes. *J. Geophys. Res.,* **90,** 6026-6032.

Jorgensen, D. P., and M. A. LeMone, 1989: Vertical velocity characteristics of oceanic convection. *J. Atmos. Sci.,* **46,** 621-640.

Knutson, T. R., K. M. Weickmann and J. E. Kutzback, 1986: Global scale intraseasonal oscillations of outgoing longwave radiation and 250 mb zonal wind during Northern Hemisphere summer. *Mon. Wea. Rev.,* **114,** 605-623.

_____, and K. M. Weikmann, 1987: 30-60 day atmospheric oscillations: Composite life cycles of convection and circulation anomalies. *Mon. Wea. Rev.,* **115,** 1407-1436.

Kousky, V. E., editor, 1993: *Climatic Diagnostics Bulletin, December 1993.* Near real time analyses: ocean/atmosphere, U.S. Department of Commerce, NOAA, Washington, DC., 79 pp.

LeMone, M. A., T. Y. Chang, and C. Lucas, 1994: On the effects of filtering on convective-core statistics. *J. Atmos. Sci.,* **51,** 3344-3350.

Lopez, R. E., and R. L. Holle, 1986: Diurnal and spatial variability of lightning activity in Northeastern Colorado and central Florida during the summer. *Mon. Wea. Rev.,* **114**, 1288-1312.

Lucas, C., and R. E. Orville, 1994: TOGA COARE; Oceanic lightning. Preprints, *Fifth Symp. on Global Change Studies and Symp. on Global Electrical Circuit, Global Change, and the Meteor. Applic. of Lightning.* Nashville, TN, Amer. Meteor. Soc., 378-382.

_____,E. J. Zipser, and M. A. LeMone, 1994a: Convective available potential energy in the environment of oceanic and continental clouds: corrections and comments. *J. Atmos. Sci.,* **51,** 3829-3830.

_____, _____, and _____, 1994b: Vertical velocity in oceanic convection off tropical Australia. *J. Atmos. Sci.,* **51,** 3183-3193.

Madden, R. A., and P. R. Julian, 1971: Detection of a 40-50 day oscillation in the zonal wind in the tropical Pacific. *J. Atmos. Sci.,* **28,** 702-708.

_____, and _____, 1972: Description of global-scale circulation cells in the tropics with a 40-50 day period. *J. Atmos. Sci.,* **29,** 1109-1123.

_____, and _____, 1994: Observations of the 40-50 day tropical oscillation -- A review. *Mon. Wea. Rev.,* **122,** 814-837.

Mapes, B. E., and R. A. Houze, Jr., 1993: Cloud clusters and superclusters over the oceanic warm pool. *Mon. Wea. Rev.,* **121**, 1398-1415.

Newton, H. J., 1988: *TIMESLAB: A Time Series Analysis Laboratory.* Wadsworth & Brooks/Cole publishing company, Advanced books and software, Pacific Grove, CA, pp. 1-92.

Orville, R. E., 1993: Lightning: Impacts and implications in aviation meteorology forecasting. Cooperative Institute for Applied Meteorological Studies, Department of Meteorology, Texas A&M University. For the second aviation weather workshop, Boulder, CO, Nov. 16-19, 1993.

_____, 1994: Cloud-to-ground lightning characteristics in the contiguous United States: 1989-1991. *J. Geophys. Res.*, **99**, 10 833-10-841.

_____, and R. W. Henderson, 1986: Global distribution of midnight lightning: September 1977 to August 1978. *Mon. Wea. Rev.*, **114**, 2640-2653.

_____, E. J. Zipser, and C. Weidman, 1994: TOGA COARE: Results from a lightning direction finder network in the remote western Pacific Ocean. Preprints, *Fifth Symp. on Global Change Studies, and Symp. on Global Electrical Circuit, Global Change, and the Meteor. Applic. of Lightning,* Nashville, TN, Amer. Meteor. Soc., 378-382.

_____, R. A., Wiesman, R. B. Pyle, R. W. Henderson, and R. E. Orville, Jr., 1987: Cloud- to-ground lightning flash characteristics from June 1984 through May 1985. *J. Geophys. Sci.*, **92,** 5640-5644.

Ramage, C. S., 1968: Role of a tropical "Maritime Continent" in the atmospheric circulation. *Mon. Wea. Rev.*, **96,** 365-370.

Randell, S. C., S. A. Rutledge, R. D. Farley, and J. H. Helsdon Jr., 1994: A modeling study on the early electrical Development of tropical convection: continental and oceanic (monsoon) storms. *Mon. Wea. Rev.*, **122,** 1852-1877.

Reap, R. M., 1986: Evaluation of cloud-to-ground lightning data from the Western United States for the 1983-1984 summer seasons. *J. Climate Appl. Meteo.*, **25**, 758-799.

_____, and D. R. MacGorman, 1989: Cloud-to-ground lightning: Climatological characteristics and relationships to model fields, radar observations, and severe local storms. *Mon. Wea. Rev.*, **117,** 518-535.

Rutledge, S. A., C. Lu, and D. R. MacGorman, 1990: Positive cloud-to-ground lightning in mesoscale convective systems. *J. Atmos. Sci.*, **47**, 2085-2100.

_____, E. R. Williams, and T. D. Keenan, 1992: The Down Under Doppler and Electricity Experiment (DUNDEE): Overview and preliminary results. *Bull. Amer. Meteor. Soc.*, **73**, 3-16.

Saunders, C. P. R., 1988: Thunderstorm electrification. *Weather,* **43,** 318-324.

Takahashi, T., 1978a: Electrical properties of oceanic tropical clouds at Ponape, Micronesia. *Mon. Wea. Rev.*, **121**, 21-35.

_____, 1978b: Riming electrification as a charge generation mechanism in thunderstorms. *J. Atmos. Sci.,* **35,** 1536-1548.

_____, 1990: Near absence of lightning in torrential rainfall producing Micronesian thunderstorms. *Geophys. Res. Letters,* **17,** 2381-2384.

Thomson, E. M., 1980: The dependence of lightning return stroke characteristics on latitude. *J. Geophys. Res.,* **85,** 1050-1056.

Uman, M. A., 1987: *The Lightning Discharge*, Academic Press, Inc., International Geophysics Series, Orlando, FL, pp. 190.

Webster, P. J., and R. Lukas, 1992: TOGA COARE: The coupled ocean-atmosphere response experiment. *Bull. Amer. Meteor. Soc.,* **73,** 1377-1416.

Williams, E. R., 1989: The tripole nature of thunderstorms. *J. Geophys. Res.,* **94,** 13 151-13 167.

_____, and R. A. Houze Jr., 1987: Satellite-observed characteristics of winter monsson cloud clusters. *Mon. Wea. Rev.,* **115**, 505-519.

_____, and N. Renno, 1993: An analysis of the conditional instability of the tropical atmosphere. *Mon. Wea. Rev.,* **121**, 21-35.

_____, R. Zhang, and J. Rydock, 1991: Mixed-phase microphysics and cloud electrification. *J. Atmos Sci.,* **48,** 2195-2203.

_____, S. A. Rutledge, S. G. Geotis, N. Renno, E. Rasmussen, and T. Rickenback, 1992: A radar and electrical study of tropical "hot towers." *J. Atmos. Sci.,* **49**, 1386-1395.

Xu, K., and K. A. Emanuel, 1989: In the tropical atmosphere conditionally unstable? *Mon. Wea. Rev.,* **117,** 1471-1479.

Zipser, E. J., 1994: Deep cumulonimbus cloud systems in the tropics with and without lightning. *Mon. Wea. Rev.,* **122**, 1837-1851.

_____, and M. A. LeMone, 1980: Cumulonimbus vertical velocity events in GATE. Part II: Synthesis and model core structure. *J. Atmos. Sci.,* **37,** 2458-2469.

VITA

Luis Alberto Rios was born on January 15, 1967 in Santurce, Puerto Rico and lived there until 1981 before moving to Oceanport, New Jersey to attend high school. After graduating from Shore Regional High School (West Long Branch, New Jersey) in 1985, he attended Rutgers University where he earned a Bachelor of Science in meteorology in 1989. In June of 1989 he joined the United States Air Force and was commissioned second lieutenant November 7, 1989. His Air Force assignments to date have included tours as a weather officer at Nellis AFB Las Vegas, Nevada; Dhahran Air Base, Dhahran, Saudi Arabia, and Lajes Field, the Azores, Portugal. He was then accepted into the Air Force Institute of Technology meteorology graduate program and to Texas A&M University in 1993 where he conducted research under the direction of Dr. Richard E. Orville.

Luis' permanent address is 84 Comanche Drive, Oceanport, New Jersey 07757.